JULY 2024

M.Sc. in Optical Engineering

KÜBRA DUMAN

REPUBLIC OF TÜRKİYE

GAZİANTEP UNIVERSITY

GRADUATE SCHOOL OF NATURAL & APPLIED SCIENCES

ASPHERIC INTRAOCULAR LENS DESIGN USING ZEMAX OPTICSTUDIO PROGRAM

M.Sc. THESIS

IN

OPTICAL ENGINEERING

BY

KÜBRA DUMAN

JULY 2024

ASPHERIC INTRAOCULAR LENS DESIGN USING ZEMAX OPTICSTUDIO PROGRAM

M.Sc. Thesis

in

Optical Engineering

Gaziantep University

Supervisor

Prof. Dr. Ahmet Necmeddin YAZICI

Co-Supervisor

Prof. Dr. Ahmet BİNGÜL

by

Kübra DUMAN

July 2024

I hereby declare that all information in this document has been obtained and presented in accordance with academic rules and ethical conduct. I also declare that, as required by these rules and conduct, I have fully cited and referenced all material and results that are not original to this work.

Kübra DUMAN

ABSTRACT

ASPHERIC INTRAOCULAR LENS DESIGN USING ZEMAX OPTICSTUDIO PROGRAM

DUMAN, Kübra
M.Sc. in Optical Engineering
Supervisor: Prof. Dr. Ahmet Necmeddin YAZICI
Co-Supervisor: Prof. Dr. Ahmet BİNGÜL
July 2024
61 pages

Nowadays; the aim of cataract surgery is not only to restore visual acuity but also to provide patients with the best quality of vision. The industrial sector for intraocular lenses (IOLs) is constantly searching for new lens models to improve the quality of vision of patients after cataract surgery. Aspheric IOLs are designed to correct the spherical aberration of the cornea. Optical quality deteriorates with increasing of eye's ages. The source of this distortion is the loss of balance between corneal aberration and lens aberration. In this study, an aspheric intraocular lens with negative spherical aberration, which compensates for the positive spherical aberration of the cornea, was designed using the Zemax OpticStudio program. A simplified human eye model was utilized for the aspheric IOL design. Compliance and performance analysis of the lens designed using the ISO Model Eye 1 as defined in the ISO 11979-2 standard was performed. The design was verified with Modulation Transfer Function (MTF) measurement results from the PMTF device. Comparative analysis between simulation results from Zemax and experimental measurements from the PMTF device demonstrated close correlation, affirming the accuracy and reliability of the optical performance analyses conducted.

Key Words: Ophthalmic optics, Intraocular lens, Lens design, Aspheric Lens, Zemax OpticStudio, MTF.

ÖZET

ZEMAX OPTICSTUDIO PROGRAMI KULLANILARAK ASFERİK GÖZİÇİ LENS TASARIMI

DUMAN, Kübra
Yüksek Lisans, Optik Mühendisliği
Danışman: Prof.Dr.Ahmet Necmeddin YAZICI
İkinci Danışman: Prof. Dr. Ahmet BİNGÜL
Temmuz 2024
61 sayfa

Günümüzde katarakt ameliyatının amacı sadece görme keskinliğini geri kazandırmak değil aynı zamanda hastalara en iyi görme kalitesini sağlamaktır. Göz içi lenslere (GİL) yönelik endüstriyel sektör, katarakt ameliyatı sonrası hastaların görme kalitesini iyileştirmek için sürekli olarak yeni lens modelleri arayışındadır. Asferik GİL'ler korneanın küresel sapmasını düzeltmek için tasarlanmıştır. Göz yaşlandıkça optik kalite bozulur; bu bozulmanın kaynağı, kornea aberasyonu ile lens aberasyonu arasındaki dengenin kaybıdır. Bu çalışmada, Zemax OpticStudio programı kullanılarak korneanın pozitif küresel aberasyonunu telafi eden, negatif küresel aberasyona sahip asferik bir göz içi lens tasarlandı. Asferik GİL tasarımı için basitleştirilmiş bir insan gözü modeli kullanıldı. ISO 11979-2 standardında tanımlanan ISO Model Eye 1 kullanılarak tasarlanan lensin uyumluluk ve performans analizi yapıldı. Tasarım, PMTF cihazından alınan Modülasyon Transfer Fonksiyonu (MTF) ölçüm sonuçlarıyla doğrulandı. Zemax'tan alınan simülasyon sonuçları ile PMTF cihazından alınan deneysel ölçümler arasındaki karşılaştırmalı analiz, yürütülen optik performans analizlerinin doğruluğunu ve güvenilirliğini teyit ederek yakın korelasyon gösterdi.

Anahtar Kelimeler: Oftalmik optik, Göziçi lens, Lens tasarımı, Asferik lens, Zemax OpticStudio, MTF.

"Dedicated to my mum"

ACKNOWLEDGEMENTS

First and foremost, I would like to express my deepest gratitude and thanks to Prof. Dr. Ahmet Necmeddin YAZICI, who has generously shared his extensive knowledge with me, provided unwavering support in every aspect, and contributed significantly to the completion of my thesis. His exemplary personality and mentorship have been invaluable throughout this journey.

I sincerely thank Prof. Dr. Ahmet BİNGÜL for his profound knowledge, guidance, and encouragement throughout my thesis process. His motivating approach significantly contributed to the development of my creative thinking processes. The guidance and knowledge imparted by him are invaluable and will remain a lifelong asset.

I would like to extend my heartfelt thanks to my visually impaired mother, Hamide KARABAŞ, who has been the primary source of inspiration for determining the topic of my thesis and conducting my research. The inspiration I received from my mother played a significant role in the selection of the thesis topic and the progression of my research. This thesis holds a unique value due to her.

Finally, I wish to express my appreciation to my loving daughter, Ece DUMAN, who was born during the course of my thesis and has been a source of endless inspiration, and to my dear husband, Çağdaş DUMAN, whose unwavering support and confidence have been invaluable. Without your support, achieving this success would not have been possible.

TABLE OF CONTENTS

LIST OF TABLES

Page

LIST OF FIGURES

Page*

LIST OF SYMBOLS

D	Diopter
mm	Millimeter
µm	Micrometer
lp/mm	Line Pairs per Millimeter
P	Power
f	Focal length
n	Refractive Index
R	Radius of Curvature
d	Thickness
λ	Wavelength
nm	Nanometer

LIST OFABBREVIATIONS

IOL	Intraocular lens
GİL	Göz içi Lens
ISO	International Organization for Standardization
MTF	Modulation Transfer Function
PMMA	Polymethyl methacrylate
ANSI	American National Standards Institute
Nd:YAG	Neodymium-doped Yttrium Aluminum Garnet
FDA	Food and Drug Administration
MICS	Microincision Cataract Surgery
PCO	Posterior Capsule Opacification
polyHEMA	Polyhydroxyethylmethacrylate
GRIN	Gradient Index
UDS	User Defined Surface
DLL	Dynamic Link Library
TRA	Transverse Ray Aberration
OPD	Optical Path Difference
USAF	United States Air Force
R&D	Research and Development

CHAPTER 1
INTRODUCTION

Approximately 20 million people worldwide are blind due to cataracts [1]. Cataract is a pathological condition where the eye lens becomes opaque, causing blurred vision, changes in color perception, halos around lights, and in severe cases, blindness. There are many causes and risk factors for the development of cataracts, but the most common cause is age-related cataracts, where the lens becomes cloudy due to aging [1]. Before the 18th century, some people believed that cataracts were caused by opaque fluid flowing from the lens, hence the etymology of cataract, which comes from the Latin "cataracta" meaning waterfall and the Greek "katarraktes" [2], [3]. When cataracts lead to visual impairment, the only treatment method available today is surgical intervention [4]. Fortunately, due to advancing technology, cataracts can now be removed and replaced with intraocular lenses (IOLs) with low complication rates. The number of intraocular lenses (IOLs) implanted to alter the eye's refractive power is doubling every year [5].

1.1 Cataract

Cataract is an ocular disease result by the clouding, hardening, and loss of transparency of the natural lens located behind the iris [6].

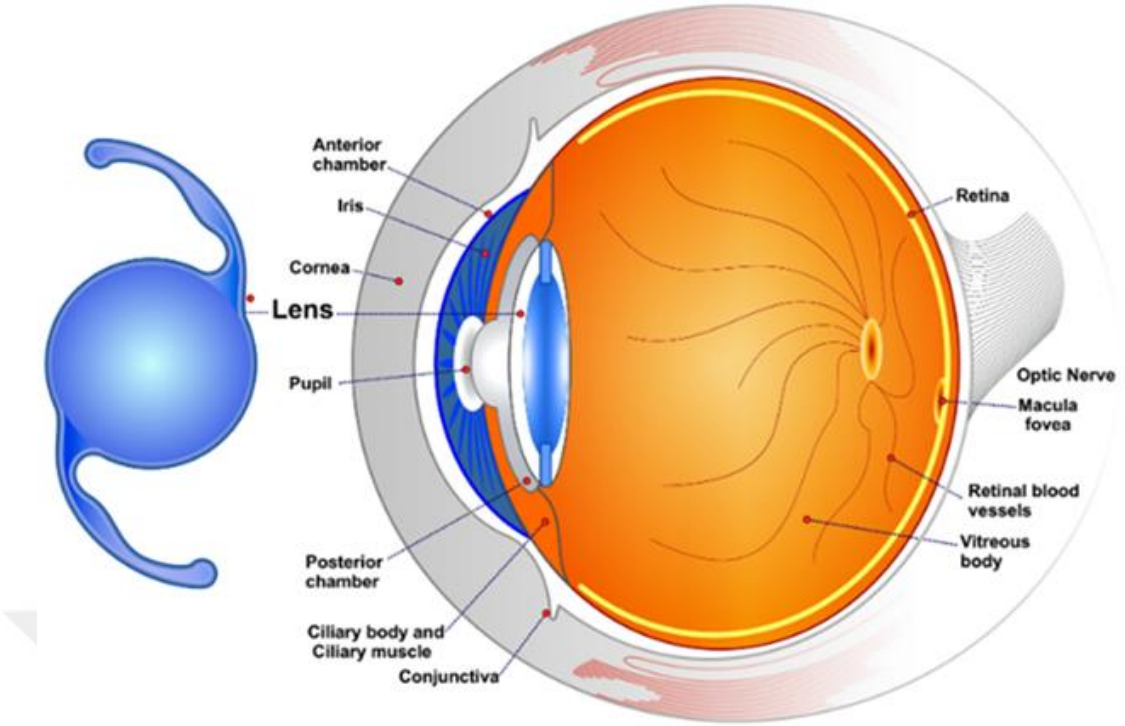

Figure 1.1 Human eye anatomy [7].

As shown in Figure 1.1 in the anatomy of the human eye, the eye consists of two lenses, the cornea and the crystalline lens, which work in concert to focus images onto the retina. The cornea, providing approximately 43 diopters of refractive power, is the outermost lens, while the iris regulates light entry. Positioned just behind the iris, the crystalline lens is responsible for focusing. The retina transforms light into neural signals, which are subsequently transmitted to the brain, resulting in visual perception. The flexible structure of the crystalline lens enables it to focus on various distances, with its refractive index being greatest at the center and gradually decreasing towards the edges. The lens alters its shape in response to muscular forces, thus enhancing its optical power [8].

The lens has been a crucial role in focusing incoming light onto the retina to produce a clear image. Cataracts impair the lens's ability to focus light on the retina, degrading the optical quality of the retinal image by reducing light transmission and scattering light, which results in symptoms such as blurred vision, decreased contrast, and glare difficulty [4]. A medical illustration depicting cataracts is shown in Figure 1.2.

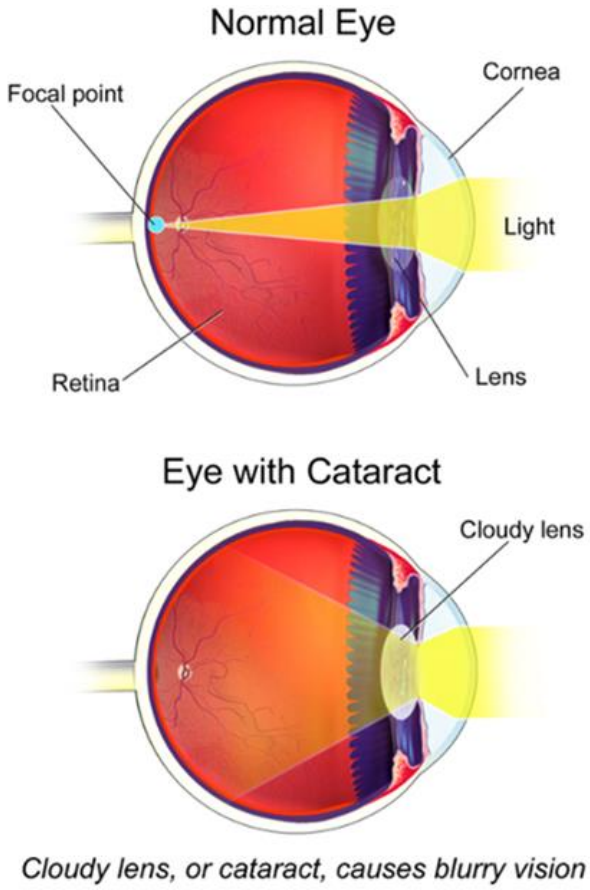

Figure 1.2 A medical illustration depicting cataracts [9].

Currently, the sole effective treatment for cataracts is surgical removal of the clouded lens, followed by the implantation of an artificial intraocular lens [2].

1.2 Cataract Surgery

Cataract surgery, also known as lens replacement surgery, involves the removal of the natural lens of the human eye, known as the "crystalline lens," which develops an opaque or cloudy area, and the insertion of an artificial intraocular lens (IOL) in its place. It is the definitive treatment for visual impairments due to lens opacification [8]. In the developed world, the most commonly preferred surgical method for cataracts is phacoemulsification [10].

Phacoemulsification, described by Charles D. Kelman in 1967, is a technique for removing cataracts whereby the lens is fragmented using an ultrasonic probe and the fragments are subsequently aspirated from the eye [11], [8], [12]. In this surgical method, ultrasonic energy is utilized to emulsify the cataract lens [12].

Phacoemulsification usually consists of six stages, as shown in Figure 1.3. These stages include:

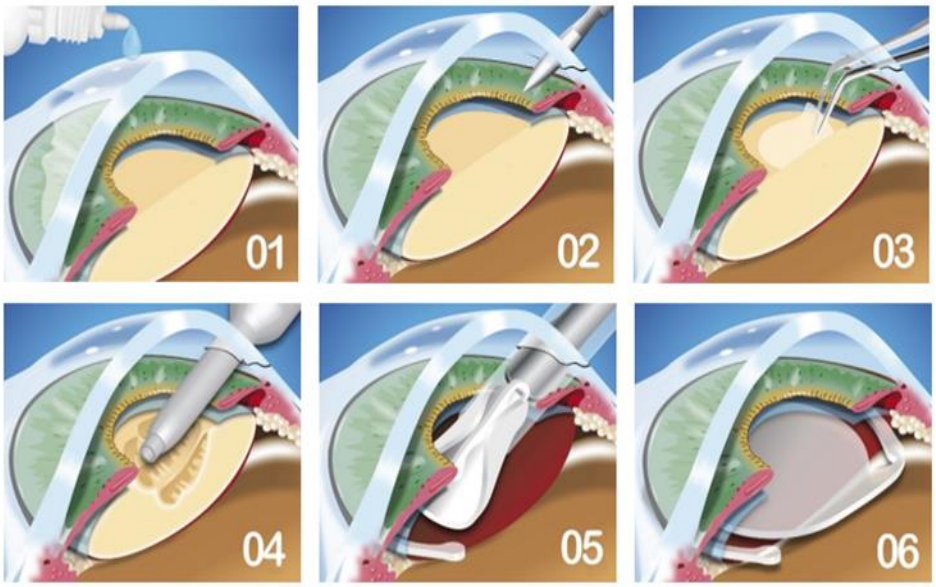

Figure 1.3 Traditional procedure of the surgery [13].

- Anesthesia – The eye is anesthetized with subtenon injection around the eye or topical anesthetic eye drops. This stage also causes paralysis of the eye muscles [12].
- Corneal incision - Two incisions are made at the edge of the transparent cornea to facilitate the insertion of instruments into the eye [12].
- Capsulorhexis - After the anterior chamber is filled with viscoelastic substance, capsulorhexis is performed [11].
- Phacoemulsification - The lens is fragmented and emulsified into liquid using the energy of ultrasonic waves from the ultrasonic probe. The resulting emulsion is removed [12].
- Irrigation and aspiration - The soft outer layer of the cataract, known as the cortex, is aspirated or absorbed. To prevent the collapse of the anterior chamber (the front portion of the eye), the fluid removed is continually replaced with a saline solution [12].
- Lens implantation - After filling the capsular bag with viscoelastic material at the incision site, the intraocular lens is inserted, followed by the aspiration of the viscoelastic material. The incision site can usually close spontaneously without the need for sutures [3], [11].

1.3 Intraocular Lens

An intraocular lens (IOL) is a surgically implanted lens in the eye used primarily for treating cataracts or correcting vision problems like myopia and hyperopia. The IOL is termed phakic if the natural lens remains in the eye; otherwise, it is referred to as a pseudophakic lens, also known as a false lens. Both types of IOLs are designed to replicate the light-focusing function of the natural crystalline lens [14].

The intraocular lens (IOL) is composed with an optic, serving as its central component, and haptic, which are side structures responsible for maintaining the lens within the capsular bag, as shown in Figure 1.4. Initially, intraocular lenses (IOLs) were made from a rigid material (PMMA), but this has largely been replaced by flexible materials such as silicone and subsequently acrylic. Most of the IOLs implanted today are fixed monofocal lenses optimized for distance vision [14].

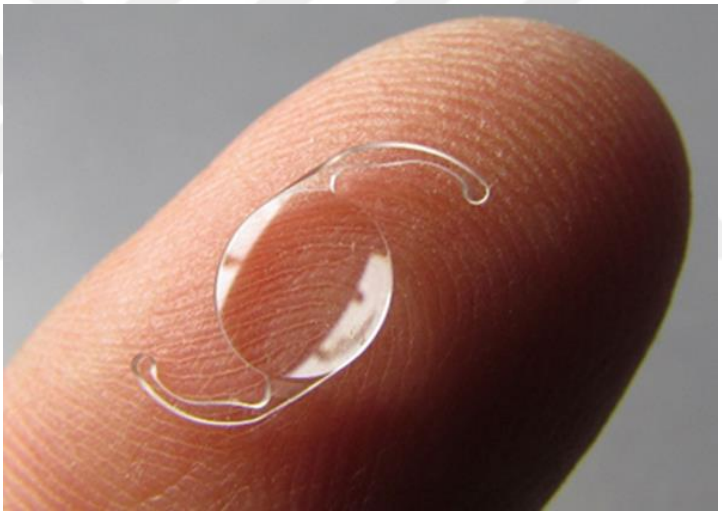

Figure 1.4 Intraocular lens [14].

IOLs are mainly utilized in cataract surgery to replace the removed crystalline lens; however, they can also be used in phakic patients solely for refractive correction. Moreover, multiple IOLs may be implanted in a single eye to achieve a specific refractive outcome. When a second IOL is positioned atop another IOL, it is termed a "piggyback lens" [15].

1.3.1 Intraocular Lens History

Cataract surgery dates back to 3000 years ago. However, the use of intraocular lenses (IOLs) was initiated by Sir Harold Ridley in 1949 [16]. During World War II, Sir Harold Ridley, an eye doctor in London, witnessed the injuries of pilots in the Royal

Air Force [17]. When aircraft were damaged during the war, fragments of the canopy of warplanes were penetrating the pilots' eyes [17], [8]. The canopies of British warplanes were made with a newly developed polymer called polymethyl methacrylate (PMMA), known as Perspex [8].

Ridley made an important observation while treating these aviators: the PMMA canopy fragments that lodged in the pilots' eyes caused little to no inflammation in the eye tissue. This was contrary to the known biological responses, as the body typically exhibited a strong inflammatory reaction to foreign objects. The biocompatibility of PMMA inspired Ridley to consider using this material in the treatment of cataracts [8].

Until that time, cataract surgeries resulted in aphakia (the absence of the lens), significantly impairing patients' vision. Aphakic patients were compelled to use thick-lensed glasses to correct their vision, presenting considerable aesthetic and practical challenges [16]. Ridley, taking advantage of the biocompatible properties of PMMA, foresaw that an artificial lens (IOL) made from this material could be implanted into the eye [8].

With this idea, Ridley performed the first IOL implantation on November 29, 1949, at St Thomas Hospital in London. The surgery was conducted on a 45-year-old female patient [17]. Ridley used a PMMA lens designed to resemble the natural lens of the human eye, with a diameter of 8.32 mm and a power of +24D [18]. Following the surgery, the patient developed myopia of 14D instead of the expected hyperopia typically seen in afakic patients [8]. Although this result indicated that the lens power was not accurately adjusted, it proved that an artificial lens could be successfully implanted into the eye.

The error in the power of the IOL stemmed from modeling the implant after the natural crystalline lens. [8] The approximate curvature radius of the crystalline lens was used for the implant, neglecting the higher refractive index of PMMA [8]. Ridley's second surgery at Moorfields Hospital in 1950 resulted in a similarly myopic outcome. However, with the third surgery, the IOL power was properly refined, leaving the patient with mild myopia [17].

While Ridley's invention was expected to generate significant excitement within the medical community, it actually encountered considerable resistance. Medical authorities of the time and many prominent ophthalmologists opposed the idea of implanting artificial lenses into the eye, arguing that such surgeries were dangerous and unnecessary. Consequently, Ridley faced professional isolation and severe criticism. This hostile attitude significantly delayed the development and widespread adoption of implant technology for decades [8].

Despite all these challenges, Ridley never lost faith in the potential of IOL technology. Over time, his efforts and accomplishments began to gain more recognition. From the mid-1970s onwards, there was increasing research and development aimed at better stabilizing and accommodating intraocular lenses within the eye. The design and materials used in the manufacture of intraocular lenses were continually improved. In 1981, the U.S. Food and Drug Administration (FDA) granted approval for IOL implantation following cataract surgery. This marked a significant milestone in the widespread acceptance of intraocular lens technology [8].

In the following years, there has been a shift in the materials used for intraocular lenses implanted into the eye, transitioning to materials that allow for easier insertion into the eye and result in fewer complications post-surgery [10]. The implantation of foldable intraocular lenses was first performed by Thomas Mazzocco in 1986. Foldable lenses are frequently used today due to their ability to be inserted through smaller incisions and their association with reduced postoperative complications [16].

1.3.2 Intraocular Lens Materials

Intraocular lens (IOL) materials are classified based on their foldability into two main types. The first material used for IOLs was PMMA (polymethyl methacrylate), which is non-foldable. Subsequently, foldable materials like silicone and acrylic were developed. Acrylic lenses can be further divided into hydrophilic and hydrophobic materials. In the early years of IOL implantation, PMMA IOLs were predominantly used [16].

PMMA lenses have advantages such as high optical resolution, a wide range of diopter options, and high intraocular stability. However, as surgical techniques evolved and incisions became smaller, the use of PMMA lenses decreased [16].

In 1984, foldable silicone lenses were introduced. While these lenses are easy to fold, their low refractive index means that they become thicker at higher diopters, complicating their use. Additionally, the posterior surface of silicone lenses can become opaque when interacting with gases in the vitreous humor [16].

Acrylic IOLs, compared to silicone lenses, cause less posterior capsular opacification. They offer advantages such as greater resistance to Nd-YAG lasers, thinner profiles due to their high refractive index, superior optical quality, and better resistance to capsular trauma because they unfold more slowly. These benefits have made acrylic lenses the most commonly used IOL material today [16].

Hydrophobic acrylic lenses should be implanted using an injector system to avoid surface trauma. Their high adhesion to the posterior capsule and sharp edges reduce the risk of opacification. On the other hand, hydrophilic acrylic lenses are more resistant to surface trauma but have a higher risk of causing posterior capsular opacification compared to hydrophobic acrylic lenses [16].

Polymethyl methacrylate (PMMA): Lenses made from polymethyl methacrylate (PMMA) material have a water content of less than 1% and a rigid and non-foldable structure [16]. With a refractive index of 1.49 and an optical diameter generally ranging from 5 to 7 mm, these lenses are non-foldable and therefore cannot pass through the small incisions used in phacoemulsification procedures [19]. Due to their typically single-piece design and large size, the use of PMMA intraocular lenses has significantly decreased in modern practice [16].

Silicone: Silicone intraocular lenses (IOLs) were developed to facilitate implantation through incisions smaller than the optic diameter [16], [19]. Silicone is a hydrophobic material of refractive index 1.41–1.46 and the optic diameter of 5.5–6.5 mm. The disadvantage of silicone is an abrupt opening in the anterior chamber following implantation which may cause rupture of the posterior capsule.

Nowadays the silicone IOLs are less commonly utilized due to their incompatibility with microincision cataract surgery (MICS) [19].

Hydrophobic foldable acrylic: Hydrophobic acrylic intraocular lenses (IOLs) represent the modern foldable IOLs that are extensively utilized today. These lenses are crafted from copolymers of acrylate and methacrylate, which are derivatives of PMMA. They are preferred due to their ease of manipulation during surgery and their ability to quickly revert to their original shape [16]. These lenses, which can be clear or colored (yellow), typically have optical diameters ranging from 5.5 to 7 mm and total lengths of 12 to 13 mm. Their refractive indices range from 1.44 to 1.55. They can be easily implanted through incisions no larger than 2.2 mm. However, due to their low self-centering capability, precise positioning is required. The risk of posterior capsule opacification (PCO) is lower compared to PMMA but higher than that associated with silicone lenses [19].

Hydrophilic foldable acrylic: Hydrophilic foldable acrylic lenses are composed of a mixture of hydroxyethylmethacrylate (polyHEMA) and hydrophilic acrylic monomer [16]. With a refractive index of 1.43 and a water content ranging from 18 to 34%, they possess a soft, compressible nature and exhibit excellent biocompatibility due to their hydrophilic surface [19]. Their small incision requirement, usually less than 2 mm, makes them ideal for microincision cataract surgery (MICS) [16]. The folding behavior of poly-HEMA chains depends on hydration levels, influencing the physical and optical properties of the polymer as water content varies. Upon hydration, these lenses absorb water, becoming soft and transparent. Among its disadvantages are a higher rate of opacification compared to other lens materials and lower resistance to capsular bag contraction [19].

1.3.3 Intraocular Lens Aberrations

In optical systems, the deviation of light from the position necessary to form the correct image is referred to as aberration [16]. Spherical aberration occurs when the refraction of light by the cornea is not uniform across its central, paracentral, and peripheral regions. The human cornea typically exhibits positive spherical aberration, whereas the natural crystalline lens compensates with inherent negative spherical aberration, resulting in low levels of positive spherical aberration in the whole eye. The crystalline lens has negative spherical aberration through its gradient index

structure and aspheric anterior and posterior surfaces. With advancing age, the spherical aberration of the lens changes towards the positive direction, and along with the cornea, spherical aberration increases positively [20].

Traditionally, intraocular lenses (IOLs) have spherical surfaces due to ease of manufacture. Since corneal spherical aberration is typically positive, spherical-surfaced IOLs cannot fully compensate for it. Therefore, aspheric IOLs are crucial for minimizing total ocular spherical aberration [16].

1.3.4 Aspheric Intraocular Lenses

The term "aspheric" is used to describe a surface that does not have a spherical shape. An aspheric lens does not converge rays from the center and the periphery at the same point, as shown in Figure 1.5. The normal human cornea is somewhat curved at the center and flatter at the periphery, a shape known as a prolate cornea. In a prolate cornea, rays from the center converge in front of those from the periphery, a phenomenon referred to as negative spherical aberration. In certain corneal disorders or following corneal surgeries, the cornea can become oblate, causing central rays to focus further back, resulting in positive spherical aberration [10].

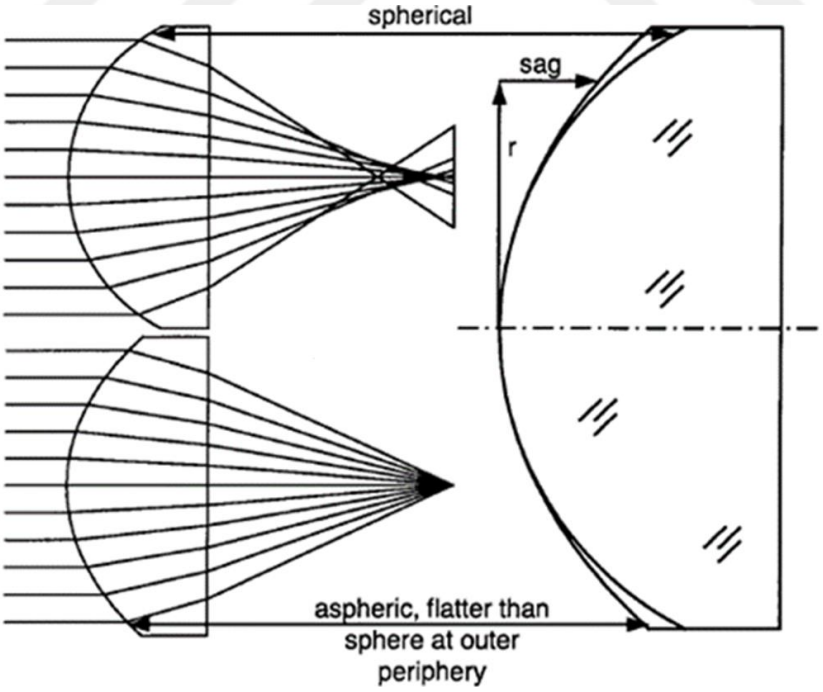

Figure 1.5 Comparison of a spherical and an aspheric lens [21].

Throughout a person's life, the normal anterior corneal spherical aberration remains constant, ranging from +0.27 μm to +0.30 μm. The natural crystalline lens counterbalances this with a negative aberration of -0.20 μm, leaving an overall positive spherical aberration of approximately +0.10 μm. As cataracts develop, positive spherical aberration increases, diminishing visual quality. Post-cataract surgery, the positive spherical aberration of the cornea persists. Aspheric intraocular lenses (IOLs) are designed to counteract this aberration with their inherent negative spherical aberration, thereby balancing the cornea's positive spherical aberration. However, for optimal function, the intraocular lens must be positioned correctly within the eye [10].

1.4 Modulation Transfer Function (MTF)

Modulation Transfer Function (MTF) may be the most comprehensive criteria for evaluating the performance of optical systems, particularly those involved in image formation [21]. It represents the ability of an optical system to convey various levels of detail (spatial frequency) of an object to form an image. This function is essential for measuring and evaluating the optical quality of intraocular lenses in vitro [10].

MTF, quantifies the capacity of a lens to convey the contrast of an object onto an image through spatial frequency, which denotes the resolution in terms of the number of line pairs per millimeter (lp/mm). Typically, MTF assessment involves employing charts comprising regularly spaced black and white lines, as depicted in Figure 1.6, to gauge the lens's performance. Subsequently, the contrast values are graphically represented against the spatial frequency on an MTF chart, exemplified in Figure 1.7 [22].

Figure 1.6 Examples of different spatial frequencies [22].

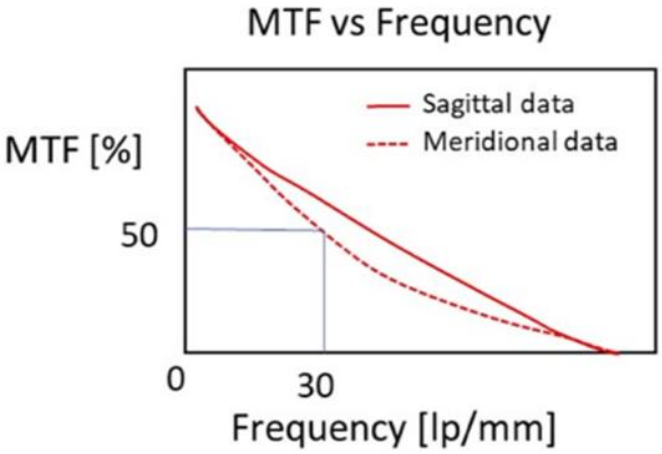

Figure 1.7 Example MTF chart showing contrast (MTF) vs. spatial frequency. The chart shows 50% contrast at a spatial frequency of 30 lp/mm [22].

Contrast is synonymous with modulation and is calculated as follows:

$$Modulation = \frac{I_{max} - I_{min}}{I_{max} + I_{min}} \tag{1.1}$$

$$MTF = \frac{\text{modulation in image}}{\text{modulation in object}} \tag{1.2}$$

Modulation is simply defined as the difference between the maximum and minimum intensities, divided by the sum of the maximum and minimum intensities, as shown in Equation 1.1. The Modulation Transfer Function (MTF), as described in Equation 1.2, is the ratio of the modulation in the image to the modulation in the object, expressed as a function of spatial frequency. Therefore, the MTF represents how well a lens transfers modulation from the object to the image across different spatial frequencies [21]. The typical MTF curve is shown in Figure 1.8.

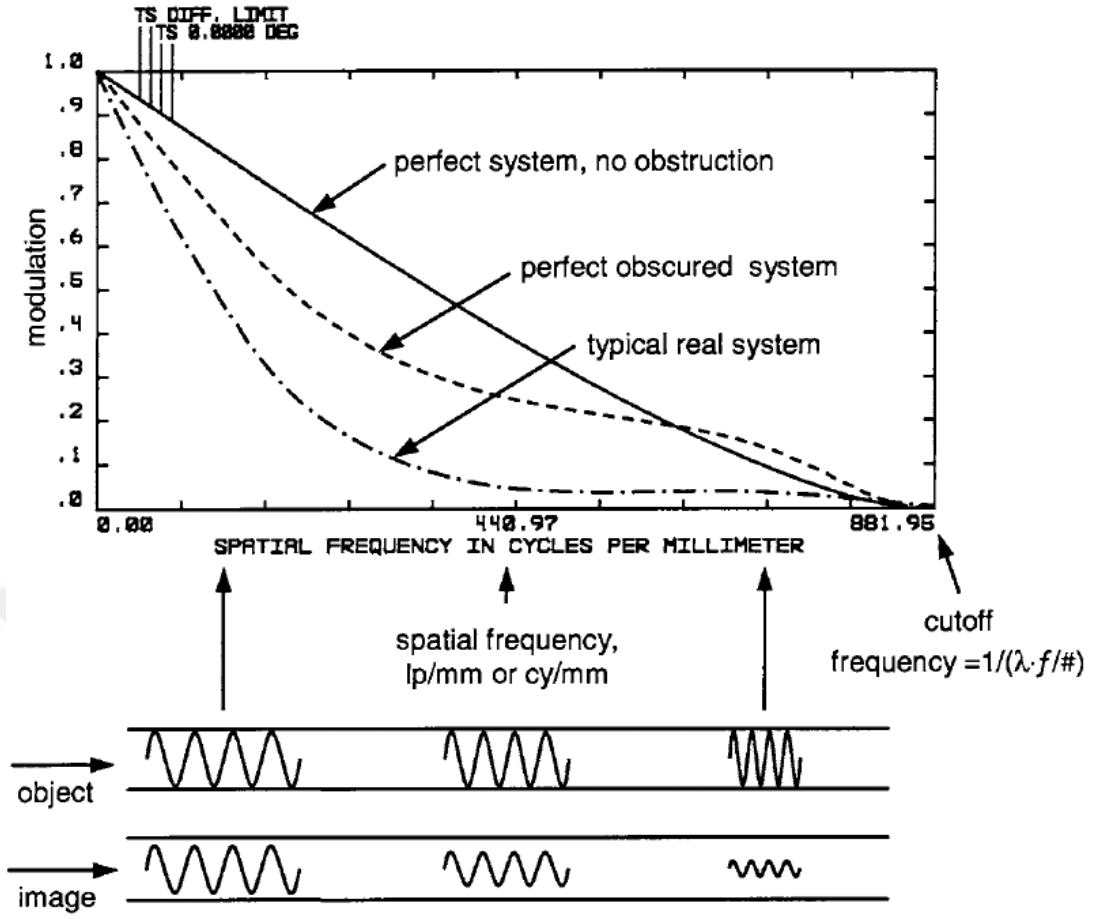

Figure 1.8 Typical MTF curves [21].

MTF serves as a critical and widely used measurement in evaluating the design and image quality of intraocular lenses. According to the EN/ISO-11979-2 standards for the imaging quality of intraocular lenses (IOLs), an MTF above 0.43 at a spatial frequency of 100 lp/mm is required for all monofocal IOLs when using an aperture of 3.0 mm in diameter. If the lens design (e.g., spherical designs) permits only smaller values, the MTF at 100 lp/mm must be at least 70% of the theoretically possible value for that specific design. In no case should the MTF at 100 lp/mm fall below 0.28 [23].

1.5 Spot Diagram

Spot diagrams are an essential analytical tool in the field of optics, providing a detailed visualization of the effects of various aberrations on image quality. By tracing a bundle of rays emanating from an object and passing through an optical system, spot diagrams plot the position of each ray on a diagram representing the image plane [24].

It is generated by calculating the intersection points on the image plane for a large set of rays. The size and shape of this geometrical ray spot can then be used to predict the quality of the design and to identify the aberrations that limit the performance of the system, as shown in Figure 1.9 [25].

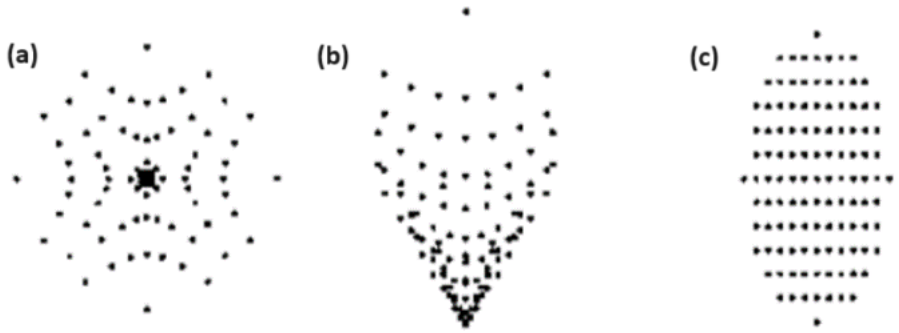

Figure 1.9 Spot diagrams for a system with a) spherical aberration b) coma c) astigmatism [25].

Through an analysis of the spots' distribution on the diagram, it becomes possible to evaluate the optical system's image quality [24].

In an ideal optical system, rays from a single object point would converge precisely onto the image plane, forming a well-defined, sharp spot. A sharp and focused spot pattern indicates minimal aberrations, while spread-out or distorted spots highlight specific optical imperfections.

They are significant in both optimizing the design of optical systems and identifying and rectifying issues in existing systems [24].

1.6 Transverse Ray Fan

Rays indicate the direction of wave-front propagation and align with the normal to the wave-front surface, which can be determined as the gradient of the wave-front. The "transverse ray aberration" (TRA) is defined as the orthogonal distance between a paraxial ray and its corresponding real ray, representing the transverse distance between the ideal and actual ray positions [26].

Ray aberration curves, also referred to as ray trace curves, quantify the linear deviation of rays from the focal point, enabling the identification and measurement of various aberrations. These curves exist in two forms: longitudinal and transverse.

Longitudinal ray aberration curves measure the distance between the aberrated chief ray and the focal point, while transverse ray aberration curves measure the distance between the focal point and the ray height above or below it in the focal plane, as depicted in Figure 1.10 [27].

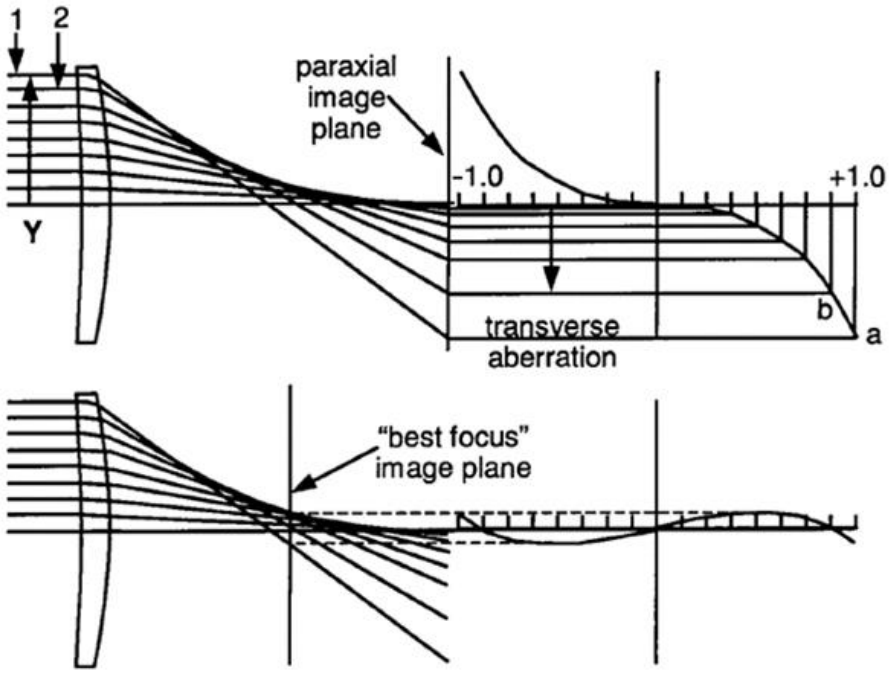

Figure 1.10 Formation of raytrace curves for spherical aberration [21].

1.7 Optical Path Difference (OPD)

Optical Path Difference is an exceptionally useful parameter for evaluating the performance of imaging optical systems [28]. Modern methods utilize OPD diagrams to describe optical system performance, particularly in terms of color correction. Geometrically perfect imagery occurs when wavefronts converging to a point image are spherical, concentric, and centered at that point for a given field of view. OPD, as depicted in Figure 1.11 measures the deviation between the real wavefront and an ideal spherical reference wavefront, which is chosen to closely match the aberrated wavefront [21].

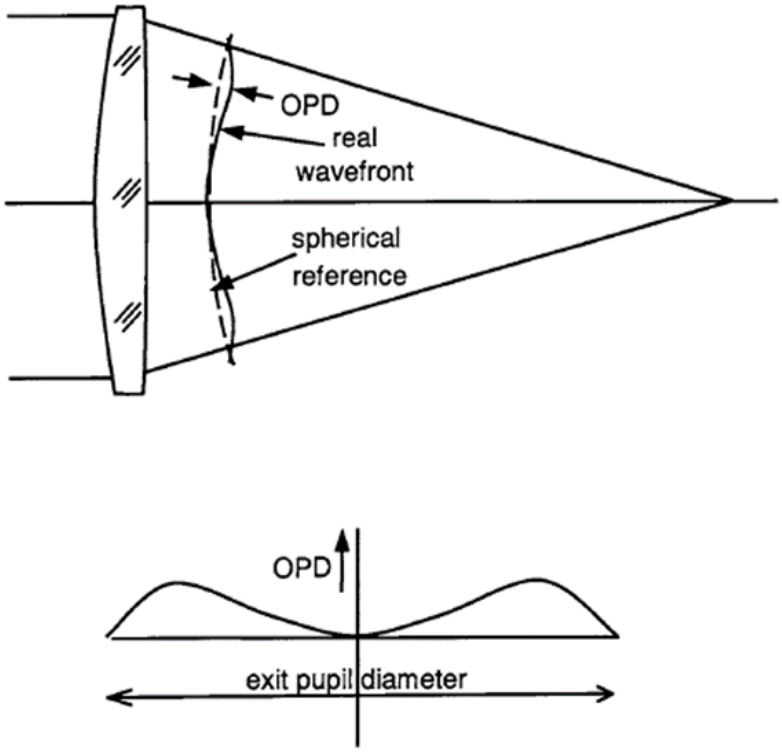

Figure 1.11 Optical path difference (OPD) [21].

The significance of OPD is highlighted by the Rayleigh criterion. According to this criterion, an optical system will perform nearly as well as a perfect system if the path length difference to a selected focus point does not exceed one-quarter of a wavelength. This implies that if the OPD is less than or equal to one-quarter of the wavelength, the system's performance will be virtually indistinguishable from perfection, producing an almost ideal Airy disk image. At this level, the central maximum and the first bright ring of the Airy disk remain qualitatively intact. However, when the OPD reaches 0.5 wavelength or more, the image quality noticeably degrades [21].

CHAPTER 2
LITERATURE SURVEY

2.1 Literature Review

The historical interest in the physiological aspects and optical properties of the living human eye, alongside their correlation with visual acuity, has roots in antiquity [20]. Recent advancements in ophthalmic technology now allow for precise and customized manipulation of human eye components, including the anterior cornea and lens. This technology opens up possibilities to utilize specific eye characteristics for improving methods of correcting optical aberrations. Nowadays, software is available that allows the design and simulation of virtually any mechanical or optical characteristic of a product before it enters the production line [29]. For current analyses, software such as Opticstudio Zemax (www.ansys.com), Code-V (www.opticalres.com), and OSLO (www.lambdares.com) are used. In this thesis study, based on our previous experiences, we have chosen to use the Opticstudio Zemax program.

Although generally similar in form, different human eye models simulate image formation by considering various combinations of properties in the constitutive elements of the eye structure (such as refractive index and surface curvatures), resulting in retinal images that closely resemble those of the biological eye [29].

2.2 Types of Eye Models

Since ancient times, there has been a longstanding interest in understanding the physiological and optical characteristics of the human eye in vivo and their connection to visual acuity. Following Gauss's seminal work in 1841, which established fundamental laws governing image formation, numerous theoretical models have been proposed. These models predominantly focus on optical properties and do not account for neurovisual effects [20].

In the late 19th century, Helmholtz conducted an extensive study on this subject, resulting in the publication of the influential Helmholtz Treatise on Physiological

Optics. Subsequently, Laurance modified Helmholtz's model, creating the Helmholtz-Laurance eye model (Figure 2.1), which includes all optical surfaces present in the human eye. Even though this model assigns refractive indices to eye components that may not precisely match measured values, its general features closely resemble those of a biological eye [20].

Helmholtz-Laurance (1909)

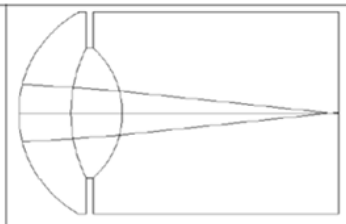

Surface	Radius (mm)	Thickness (mm)	Refraction index
1	8.0	3.6	1.333
2	10.0	3.6	1.450
3	-6.0	15.18	1.333

Figure 2.1 Helmholtz-Laurance eye model schematic [20].

Allvar Gullstrand, a Swedish Ophthalmologist, conducted significant research in physiology, particularly regarding the eye's optical properties. He was awarded the Nobel Prize in 1911 for this work. Gullstrand's eye model, while initially resembling the simplified schematic eye proposed by Helmholtz-Laurence, introduces a non-simplified version, considering the cornea to have two refracting surfaces instead of one. This improves the formation of images on the retina. Even though this model simplifies other components like the vitreous and aqueous humor, it includes the anterior and posterior surfaces of the crystalline lens, making it particularly useful for calculating intraocular lens power [20].

Gullstrand's eye model (Figure 2.2) accounts for the spherical aberration of the cornea by adjusting the axial length so that the paraxial focus aligns with the retina. Despite the sophistication of Gullstrand's model, the Emsley schematic eye, featuring only one refractive surface, remains popular in introductory courses in optometry, ophthalmology, and vision science due to its simplicity [20].

Gullstrand (1911)

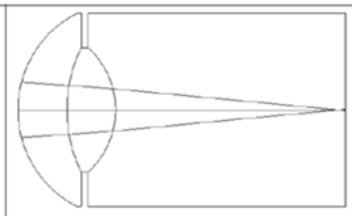

Surface	Radius (mm)	Thickness (mm)	Refraction index
1	7.8	3.6	1.336
2	10.0	3.6	1.413
3	-6.0	16.97	1.336

Figure 2.2 Gullstrand eye model schematic [20].

Lotmar pioneered the integration of aspherical surfaces into eye modeling, shaping the anterior corneal surface based on Bonnet's measurements and attributing a parabolic shape to the posterior lens surface, while maintaining spherical surfaces elsewhere. Lotmar's aspheric eye model aimed for paraxial emmetropia, calculating spherical aberration for principal rays, which aligned well with experimental data. Atchison expanded on this by developing three surface simplified emmetropic eye models using data from 106 healthy emmetropic individuals of European descent aged 18 to 69 years. This empirical model aimed to include the impact of aging on myopia, observing changes in various eye parameters with increasing age [20].

The ISO eye model, depicted in Figure 2.3, is commonly employed for reporting the performance of intraocular lenses (IOLs). Its prevalence in such evaluations is not primarily due to its accuracy or faithful depiction of the biological eye, but rather its utility as a laboratory device for physically inserting manufactured IOLs and testing prototypes. The ISO eye model, as specified in ISO 11979-2, is designed specifically to evaluate the behavior of IOLs and for comparative purposes. It does not aim to closely mimic the anatomy or optical behavior of the human eye. During testing, the examined IOL is placed in a fluid-filled enclosure chamber a physiological saline solution, simulating the intraocular environment. In most ISO tests, convergent rays from the cornea must intersect a point with a 3 mm diameter on the tested IOL, typically achieved using a 3 mm aperture positioned directly prior to the IOL [20].

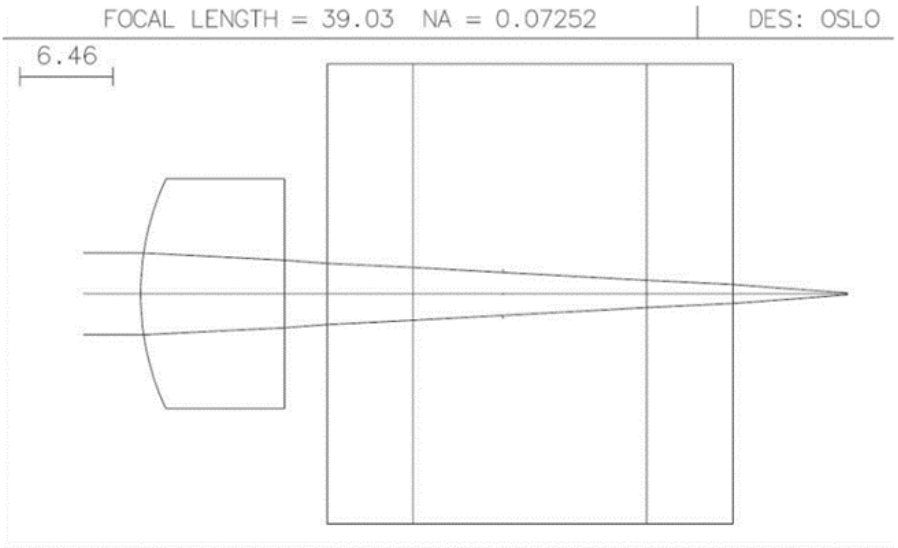

Figure 2.3 ISO eye model schematic [20].

Liou & Brennan introduced a comprehensive eye model in 1997 (Figure 2.4), regarded by some sources as the most anatomically, biometrically, and optically accurate comparison to the physiological eye. Their aim was to construct a model capable of predicting visual performance under various conditions by utilizing empirical ocular parameter values. Unlike conventional models, the Liou & Brennan eye incorporates a gradient index (GRIN) surface to simulate the human crystalline lens. However, in this particular study, the crystalline lens model is substituted with parameters of a designed intraocular lens (IOL), featuring a distinct geometry and a fixed refractive index. Moreover, the cornea in this model is represented with varying curvatures and conic constants on both its anterior and posterior surfaces [20].

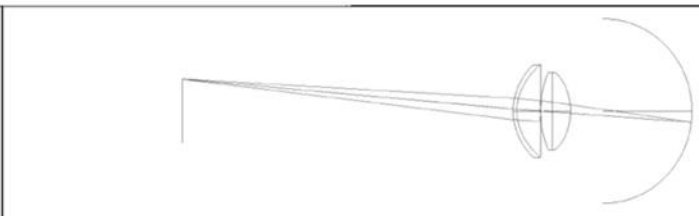

Liou and Brennan (1997)

Surface	Radius (mm)	Thickness (mm)	Asphericity	Refraction index (555nm)
1	7.77	0.50	-0.18	1.376
2	6.40	3.16	-0.60	1.336
3	12.40	1.59	-0.94	Grad A
4	Infinity	2.43	—	Grad P
5	-8.10	16.27	0.96	1.336

$GradA = 1.368 + 0.049057 \cdot z - 0.015427 \cdot z^2 - 0.001978 \cdot r^2$ $GradP = 1.407 - 0.006605 \cdot z^2 - 0.001978 \cdot r^2$

$n(\lambda) = n(0.555\mu m) + 0.0512 - 0.1455 \cdot \lambda + 0.0961 \cdot \lambda^2$

Figure 2.4 Liou-Brennan eye model schematic [20].

As part of the literature studies, a study compared the optical performances of five different schematic eye models (Helmholtz-Laurance, Gullstrand, Emsley, Greivenkamp, and Liou & Brennan) and determined which model provides the most accurate results. Simulations conducted using Zemax software were based on optical quality parameters such as Modulation Transfer Function (MTF), spot diagrams, ray fan, and Strehl Ratio. The results indicated that the Liou and Brennan model best represents the biological eye characteristics; this model features a gradient refractive index distribution and a decentered pupil [29]. These findings serve as an important reference for optical modeling and eye simulations.

Mike Tocci addressed creating a human eye model using the Liou & Brennan 1997 model in OpticStudio and designing freeform progressive eyeglass lens using this

model. In this study, the complexity of human eye modeling and the critical aspects of this process are thoroughly explained. It is detailed how to create an eye model, including components such as cornea, pupil, lens and retina, step by step in OpticStudio, and how to evaluate the performance of the model by dot diagram, MTF and diffraction image analysis. As a result, human eye modeling and eyeglass lens design are explained step by step in OpticStudio, and the accuracy of the model is verified by performance analysis [30].

In Rod Watkins' study, various human eye models are presented in OpticStudio using only glass catalog data. This article details various human eye models used in Zemax OpticStudio, important for designing and analyzing optical systems. The article includes models for retinal imaging, accommodated vision, and more, emphasizing customization based on specific needs. He provides simplified to complex models, discussing their applications in designing ophthalmic instruments and studying eye pathologies [31].

In the Hernandez study, examined the use of diffractive surfaces in modeling intraocular lenses (IOL). Diffractive IOLs provide multifocal designs that correct both distant and near vision. Utilizing Rod Watkins's human eye model, Hernandez developed a bifocal IOL. His research elucidated the mathematical models, configurations, and optimization processes employed to calculate the phase delay of diffractive surfaces [32].

Building on these studies, in thesis, we recreated the simplified human eye model presented in Rod Watkins' work in Zemax OpticStudio and aimed to design an aspheric intraocular lens on this model.

In the Timar-Fulep study, he examined how to create a realistic model of relief-type diffractive lenses using User Defined Surface (UDS) DLLs in Zemax OpticStudio, and the advantages of this model over existing diffractive surface models. In this study, modeling of an ideal bifocal diffractive IOL design using UDS DLLs yielded results consistent with theoretical expectations. The model was validated against the ISO 11979-2 standard eye model [33]. In this study, although diffractive lens design was addressed, ISO 11979-2 is a universally applied standard for all intraocular lenses. This validation approach informed our own study. Despite our work being

centered on an aspheric lens, we adopted the validation methodology used in this thesis to assess the performance and verification of our designed aspheric IOL. We conducted performance analyses by simulating our designed lens on the ISO 11979-2 eye model.

2.3 Tilt and Decentration Effect Studies

Another important factor in design is that intraocular lenses (IOLs) are typically designed to be placed within the capsular bag at a specific distance. However, their actual longitudinal positioning can vary during surgery, potentially affecting the quality of the reflected image. Additionally, an IOL may be misaligned or tilted off the primary optical axis, which can impact its overall performance [20]. It is one of the important points that should not be ignored, especially for aspheric lens design. Because aspheric lenses are very sensitive to tilt and desentration effects. This effect has become a disadvantage of aspheric lenses [34]. Therefore, when designing an aspheric IOL, analyzing and evaluating the effects of tilt and decentration is crucial. In our thesis, taking this factor into account, the effects of tilt and decentration of the designed aspheric intraocular lens have been analyzed, and the results are presented in the Appendix.

In a study conducted at the Institute of Medical Physics at the University of Erlangen-Nürnberg in Germany, the impact of decentration and tilt errors on image quality in aspheric intraocular lens (IOL) designs was examined. In this study, the optical performance of 6 different IOL designs has evaluated using a model eye. Experiments have performed using monochromatic green light at a wavelength of 555 nm and retinal position was optimized for best image quality. IOLs have placed with up to 1.0 mm decentration and up to 5 degrees of obliquity relative to the line of sight. Modulation transfer function (MTF) measurements have recorded with pupil diameters of 3.0 mm and 4.5 mm [35].

The results have demonstrated that aberration correcting IOLs are highly sensitive to decentration and tilt, but this effect varies depending on the design. Aberration-free IOLs have shown less sensitivity and provided better image quality compared to spherical IOLs over a wider range of displacements. Additionally, specific designs of aberration correcting IOLs have been found to have a significant impact on sensitivity to displacement. IOLs with anterior and posterior aspherics have been

shown to be more resistant to decentration than IOLs with single anterior aspherics. In aspheric IOL designs, it has been suggested that aberration correction be adjusted to the posterior surface or both surfaces. Overall, modern aspheric IOLs have been reported to provide superior image quality compared to traditional spherical IOL designs. It has been noted in the literature that aberration-correcting IOLs have the potential to achieve diffraction-limited image quality when properly aligned [35].

There are many different research and studies examining the decentration and tilt effects of aspheric intraocular lens (IOL) designs [34], [36], [37]. The literature presents conflicting findings regarding the impact of aspheric IOLs on visual performance compared to spherical lenses. Factors such as variations in corneal spherical aberration and the alignment, tilt, and spherical nature of the lens play significant roles in these contradictions, complicating the interpretation of results.

Monte´s-Mico´ and colleagues reviewed studies analyzing the effects of different spherical and aspheric intraocular lenses (IOLs) on vision and optical quality. This comprehensive review highlights the complexity and variability in visual and optical outcomes following the implantation of spherical and aspheric IOLs. The optical advantages of aspheric intraocular lenses have been shown to depend on specific factors such as pupil size, lens tilt, decentration, depth of focus, and certain corneal spherical aberrations. The potential benefits of aspheric lenses have been noted to be limited by factors such as incomplete or incorrect preoperative measurement of ocular parameters, manufacturing defects, incorrect placement of the lens, and post-surgical aberrations. However, studies in the literature have concluded that even in the worst-case scenarios, the optical and visual performance of aspheric lenses is equivalent to or better than that of spherical lenses [36].

CHAPTER 3
MATERIALS AND METHODS

3.1 Materials

3.1.1 PMTF System

The PMTF system is an optical device designed to provide high-precision measurements of optical power and modulation transfer function (MTF) to lens manufacturers. It has the capability to measure and characterize various types of intraocular lenses (refractive & diffractive). The PMTF performs MTF measurements in accordance with the ISO11979-2 standard [38].

The PMTF device is equipped with software that makes it suitable for the examination and characterization of IOLs in both R&D and production environments [38]. The schematic representation of the PMTF system utilized for experimental measurements provided in Figure 3.1.

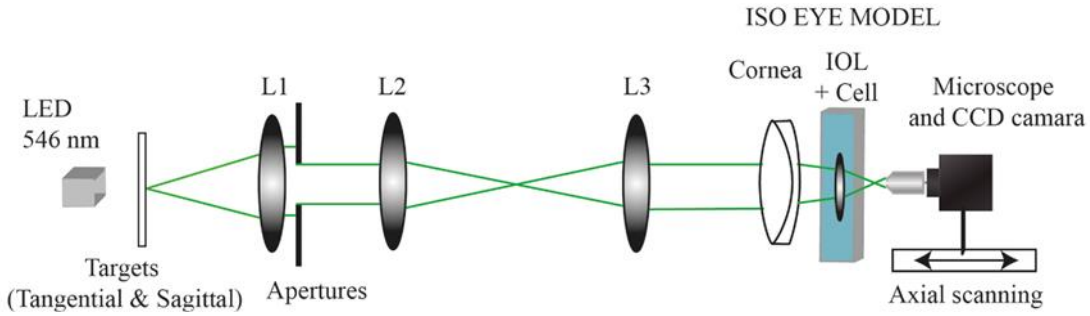

Figure 3.1 The schematic illustration of the PMTF system [34].

3.2 Methods

3.2.1 IOL Design Procedure

In the design of intraocular lenses (IOL), geometric properties such as the radius of curvature, lens thickness, material, and refractive index serve as the starting points. Understanding the lensmaker's formula is crucial in the lens design process to achieve an effective intraocular lens [20]. The diagram shown in Figure 3.2 represents a positive (converging) monofocal lens.

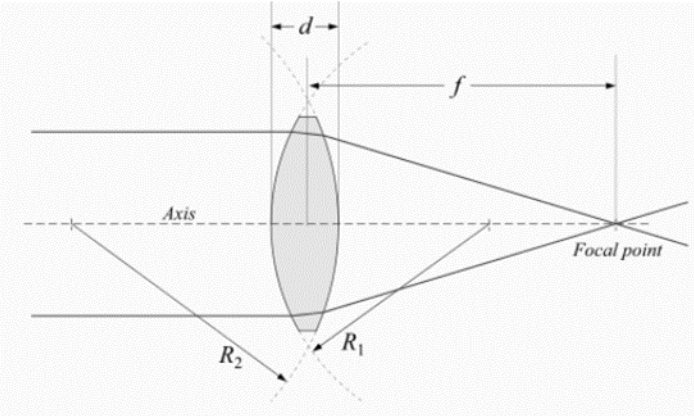

Figure 3.2 Diagram of a positive (converging) monofocal lens [39].

The focal length of a thick lens can be calculated from the lensmaker's equation, as given in Equation 3.1:

$$P = \frac{1}{f} = \left(\frac{n_{lens-n_m}}{n_m}\right) \cdot \left[\frac{1}{R_1} - \frac{1}{R_2} + \left(\frac{n_{lens} - n_m}{n_m} \cdot \frac{d}{n_{lens} R_1 R_2}\right)\right] \tag{3.1}$$

where, P denotes the optical power of the lens, f represents its focal length, n_{lens} stands for the refractive index of the lens material, n_m denotes the refractive index of the surrounding medium, R_1 and R_2 signify the radii of curvature of the anterior and posterior surfaces of the lens respectively, while d indicates the thickness of the lens.

In the design of intraocular lenses (IOL), the starting point is typically determined by the choice of diopter power. The selection of the material for the lens and the refractive index of the chosen material are also of paramount importance. The thick lens equation can be simplified further depending on design preferences. If a symmetrical biconvex IOL is preferred, the values of R_1 and R_2 will be equal. If a different biconvex IOL design is desired, the radius values may differ. In general, R_1 has a positive value and R_2 has a negative value [20].

The lens thickness can be designed not only with a focus on the desired optical performance but also considering the mass of the material and its effects when implanted into the capsular bag during surgery.

The overall design procedure is outlined as shown in Figure 3.3.

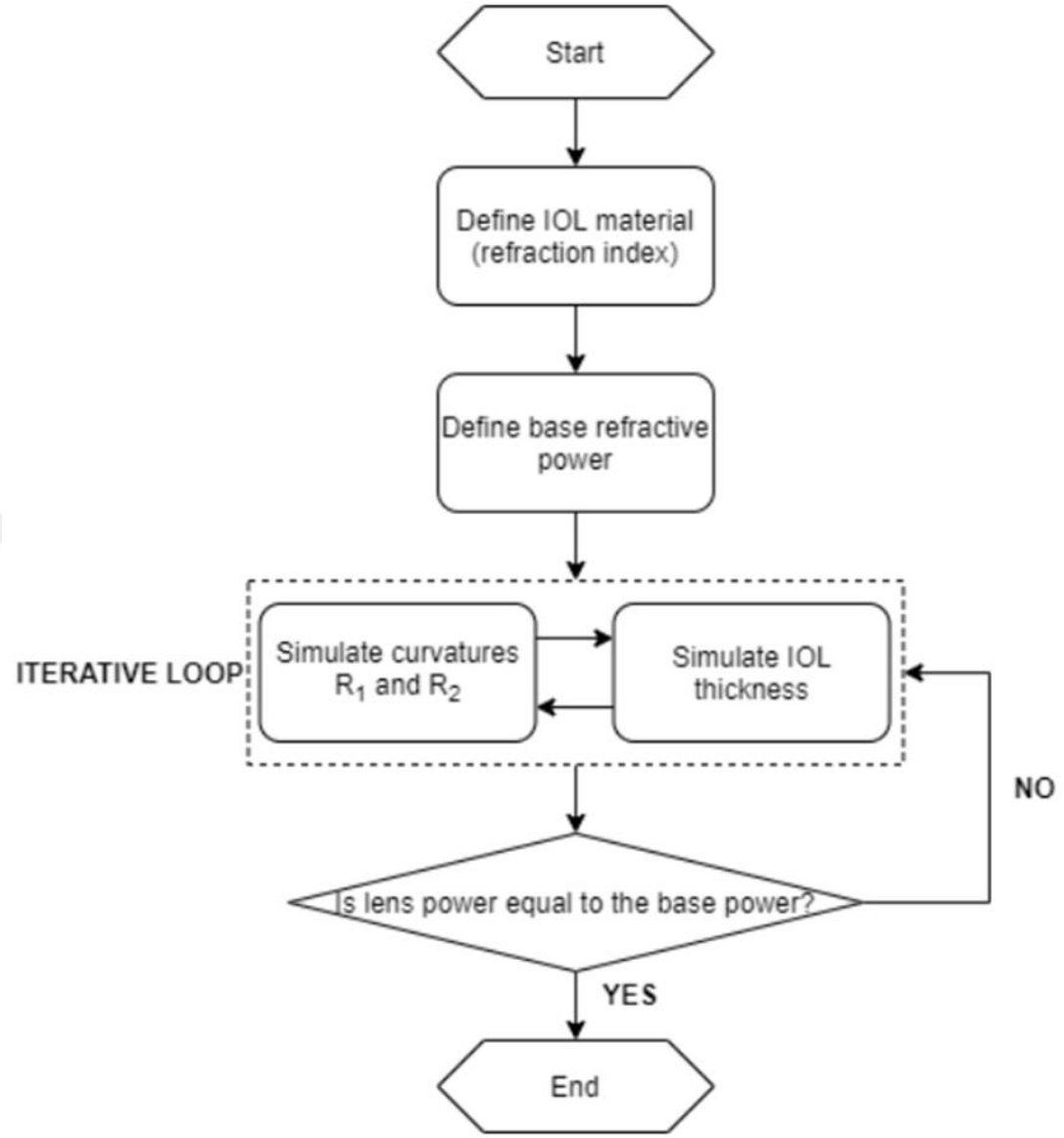

Figure 3.3 Overall design procedure for IOL design [20].

3.2.2 Aspheric IOL design on human eye model

The accurate simulation and modeling of the human eye is often a challenging process; this topic continuously encourages new developments. Within the scope of this study, the simplified human eye model based on the literature will be applied in the Zemax program. This model is quite detailed and includes realistic factors such as a balanced pupil, curved retina surface, inward-facing eyeball [31]. This eye model will be implemented in OpticStudio and used for aspheric IOL design.

The optical dimensions of intraocular lenses (IOLs) typically range between 5.25 mm and 6.50 mm, while the haptic length varies from 12.00 mm to 13.50 mm [40]. The IOL thickness is less than one millimeter [41].

In this design, the optical size of the intraocular lens is preferred to be 6.00 mm, with a haptic length of 12.00 mm, and a lens thickness of 1.00 mm. A hydrophobic acrylic material with a refractive index of n=1.48 is chosen for the lens material. As for the medium, natural saline is defined with a refractive index of n_0 = 1.336. The designed IOL will have a basic refractive power of P = +20.00 D.

The designed lens is biconvex and adjusted to provide maximum contrast for objects at infinite distance. In this study, the intraocular lens designed has both anterior and posterior aspheric surfaces.

The primary aim of this study is not to design the best aspheric intraocular lens but to demonstrate the utilization of OpticStudio Zemax program for aspheric IOL design.

Utilizing the human eye model, an aspherical IOL with +20.00 D diopter power was designed in the Zemax program. The design details and optical performance analyzes of the aspheric IOL designed using the Zemax program are as follows:
The design details of the aspheric IOL designed using the Zemax program are shown in Figure 3.4. The Zemax layout of the human eye model with the aspherical IOL design is depicted in Figure 3.5.

Lens Data

Update: All Windows

Surface 1 Properties | Configuration 1/1

	Surface Type		Comment	Radius	Thickness	Material	Clear Semi-Dia	Chip Zone	Coating	Mech Semi	Conic	TCE x 1E-6
0	OBJECT (aper)	Standard		Infinity	Infinity		Infinity U	0,000		Infinity	0,000	0,000
1		Standard		Infinity	4,000		4,068	0,000		4,068	0,000	0,000
2	(aper)	Standard	CORNEA	7,800	0,520	CORNEA	6,000 U	0,000		6,000 U	-0,500	-
3	(aper)	Standard		6,700	1,500	AQUEOUS	6,000 U	0,000		6,000 U	-0,300	-
4		Standard		11,000	1,600	AQUEOUS	11,000 U	0,000		11,000	0,000	-
5	STOP	Standard	IRIS	Infinity	0,100	AQUEOUS	1,332	0,000		1,332 U	0,000	-
6	(aper)	Standard	LENS	11,420	1,000	1,48,52,0 M	3,000 U	0,000		6,000 U	-0,270	0,000
7	(aper)	Standard		-19,480	18,784	VITREOUS	3,000 U	0,000		6,000 U	-0,270	-
8	IMAGE	Standard	RETINA	-11,000	-		11,000 U	0,000		11,000	0,000	0,000

Figure 3.4 Zemax sequential mode lens data of the human eye model with aspherical IOL design.

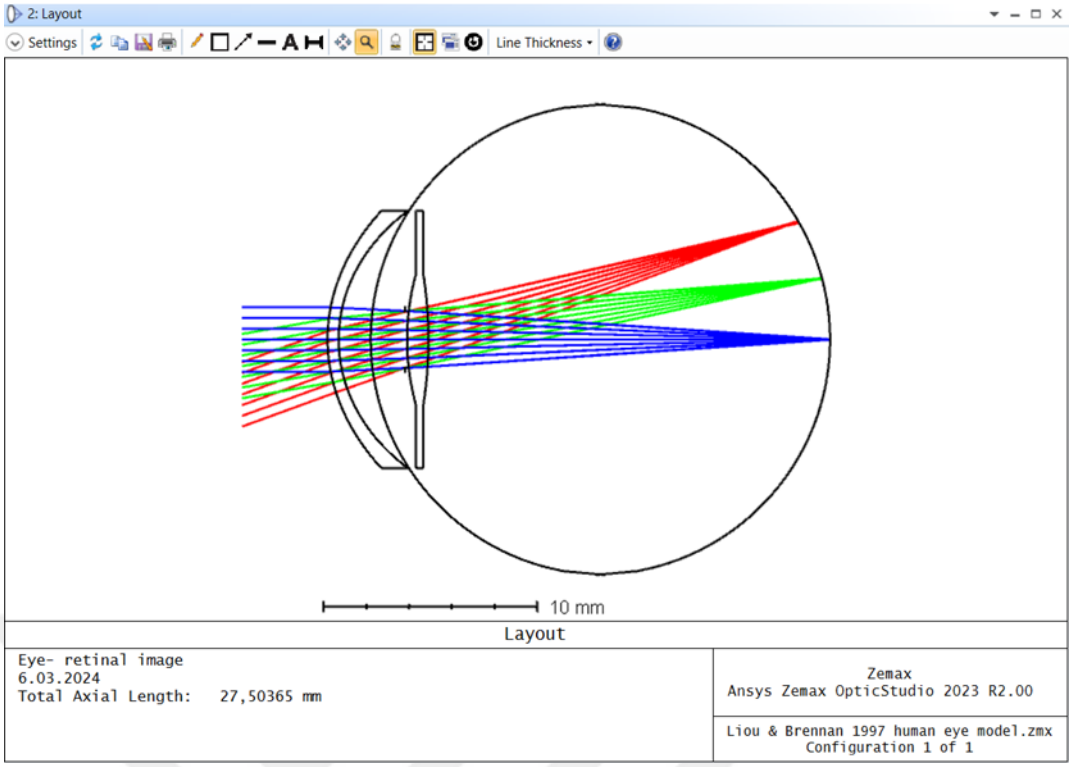

Figure 3.5 Zemax layout of the human eye model with aspherical IOL design.

The optical performance analysis of the aspheric IOL designed using the Zemax program has been conducted. The first step in analyzing this lens is to examine the MTF curve. The Zemax MTF curve of the human eye model with the aspherical IOL design for three different fields and white light is depicted in Figure 3.6. Additionally, the Zemax MTF curve of the human eye model with the aspherical IOL design at a wavelength of 0.555 μm is given in Figure 3.7.

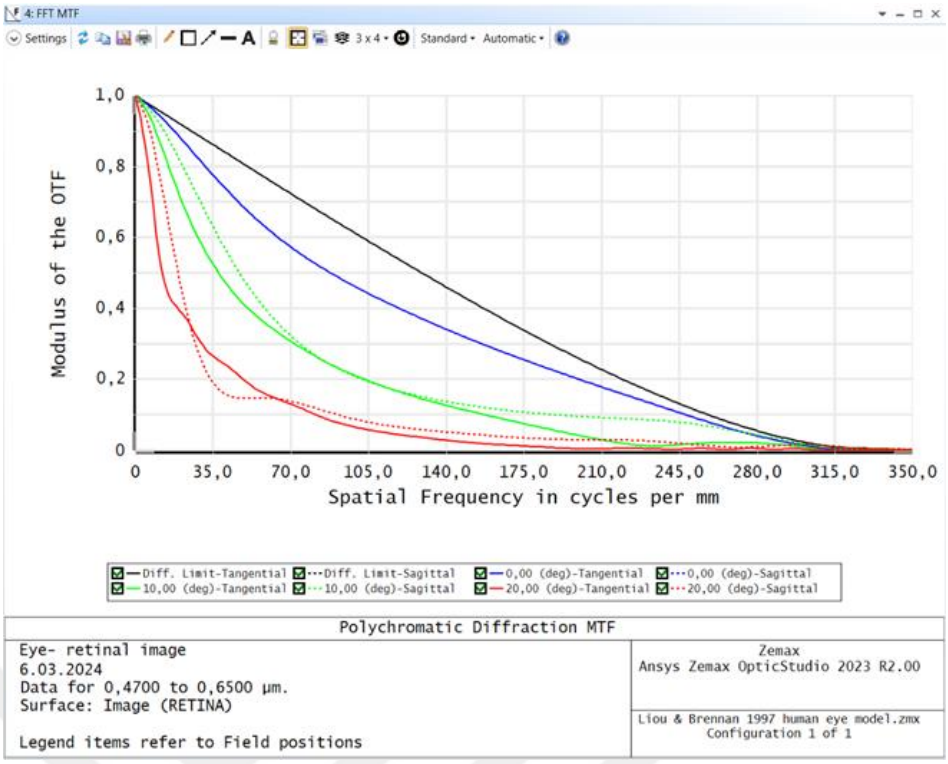

Figure 3.6 Zemax MTF curve of the human eye model with aspherical IOL design (for 3 different field and white light).

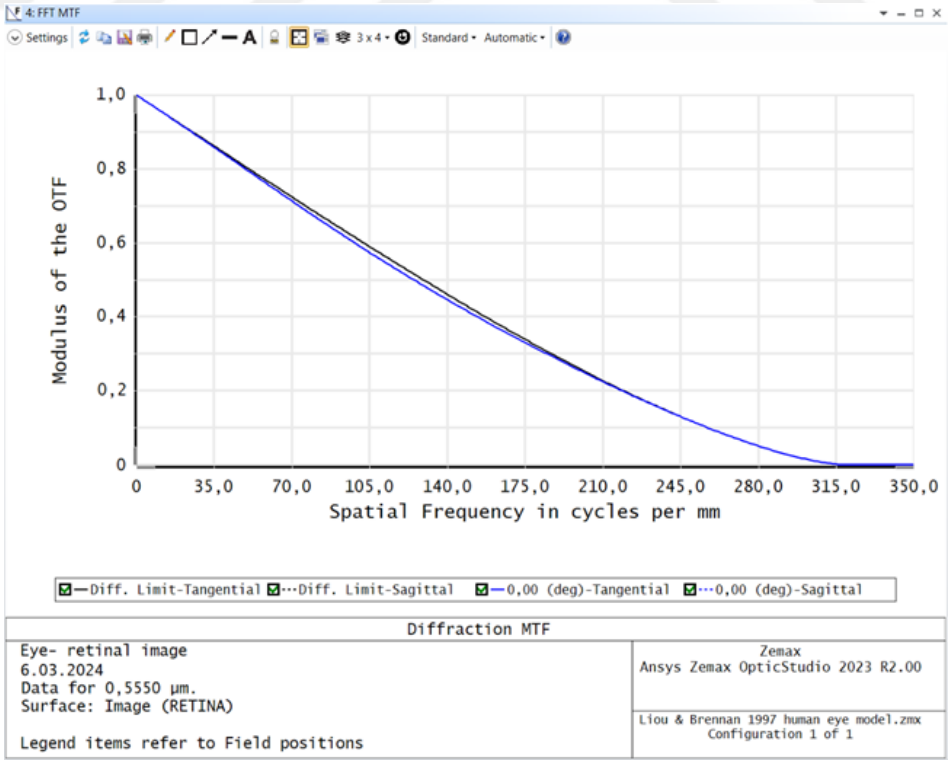

Figure 3.7 Zemax MTF curve of the human eye model with aspherical IOL design (for 0.555 µm wavelength).

Examining the spot diagram is crucial in this lens analysis. Figure 3.8 depicts the Zemax spot diagram of the human eye model with the aspherical IOL design for three different fields and white light. Furthermore, Figure 3.9 shows the Zemax spot diagram of the human eye model with the aspherical IOL design at a wavelength of 0.555 μm.

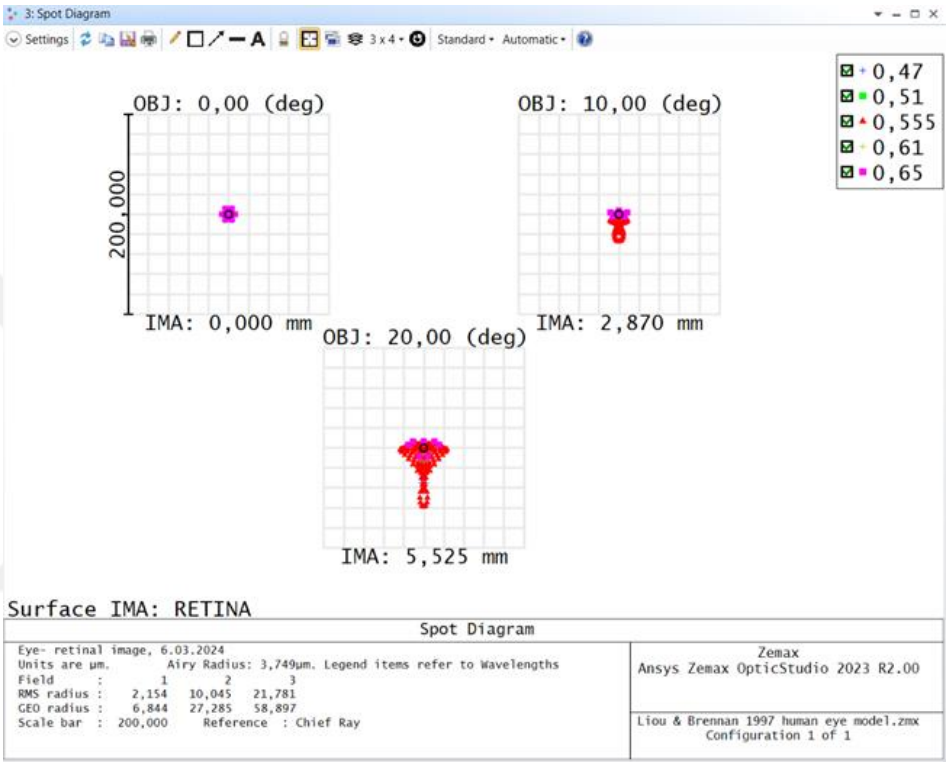

Figure 3.8 Zemax spot diagram of the human eye model with aspherical IOL design (for 3 different field and white light).

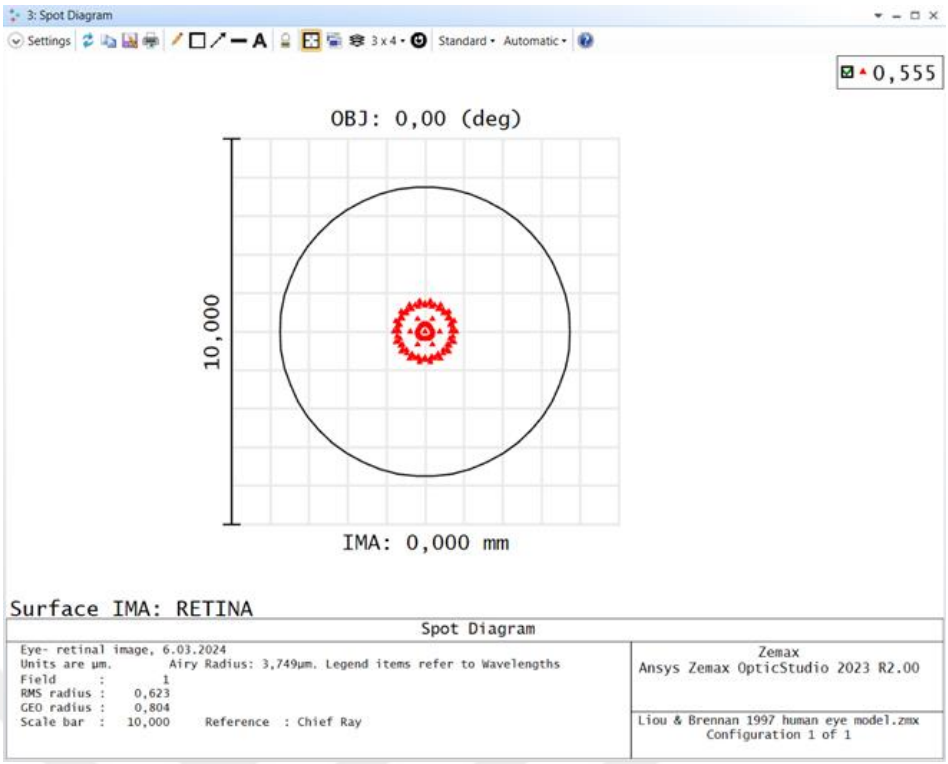

Figure 3.9 Zemax spot diagram of the human eye model with aspherical IOL design (for 0.555 µm wavelength).

Another important aspect of the analysis includes evaluating the Ray fan and Optical Path Difference (OPD) diagrams. Figure 3.10 illustrates the Zemax transverse ray fan plot for the human eye model with the aspherical IOL design under three different fields and white light conditions, while Figure 3.12 displays the corresponding Zemax OPD fan plot. Additionally, Figure 3.11 shows the Zemax transverse ray fan plot for a wavelength of 0.555 µm, and Figure 3.13 gives the corresponding Zemax OPD fan plot for the same wavelength. These analyses provide valuable insights into the optical performance and aberrations of the aspherical IOL design.

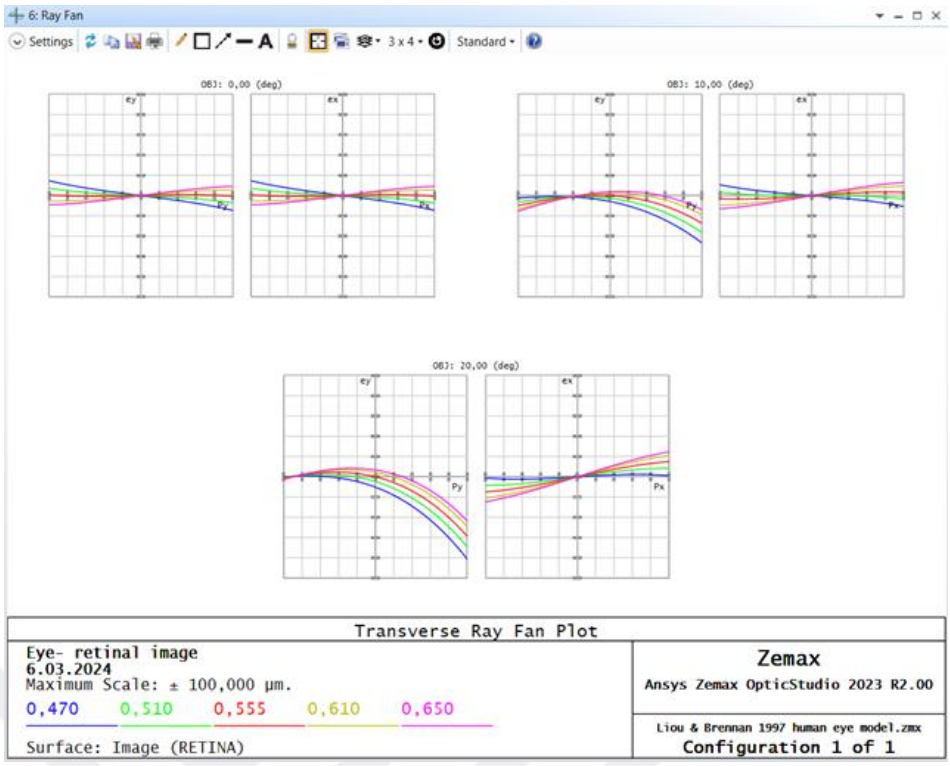

Figure 3.10 Zemax transverse ray fan plot of the human eye model with aspherical IOL design (for 3 different field and white light).

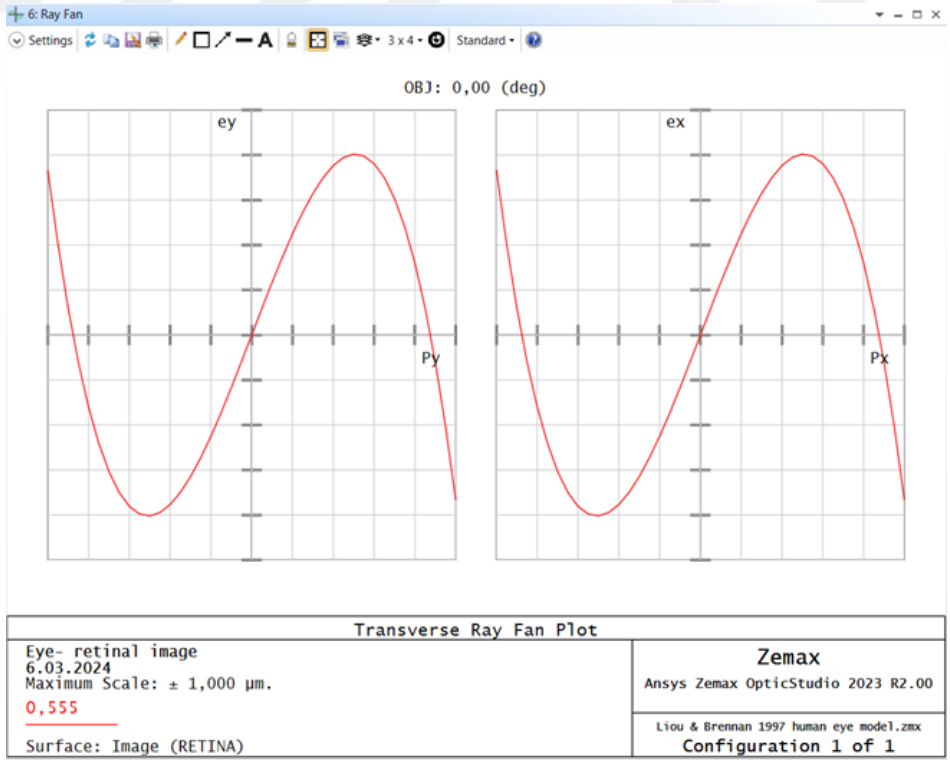

Figure 3.11 Zemax transverse ray fan plot of the human eye model with aspherical IOL design (for 0.555 µm wavelength).

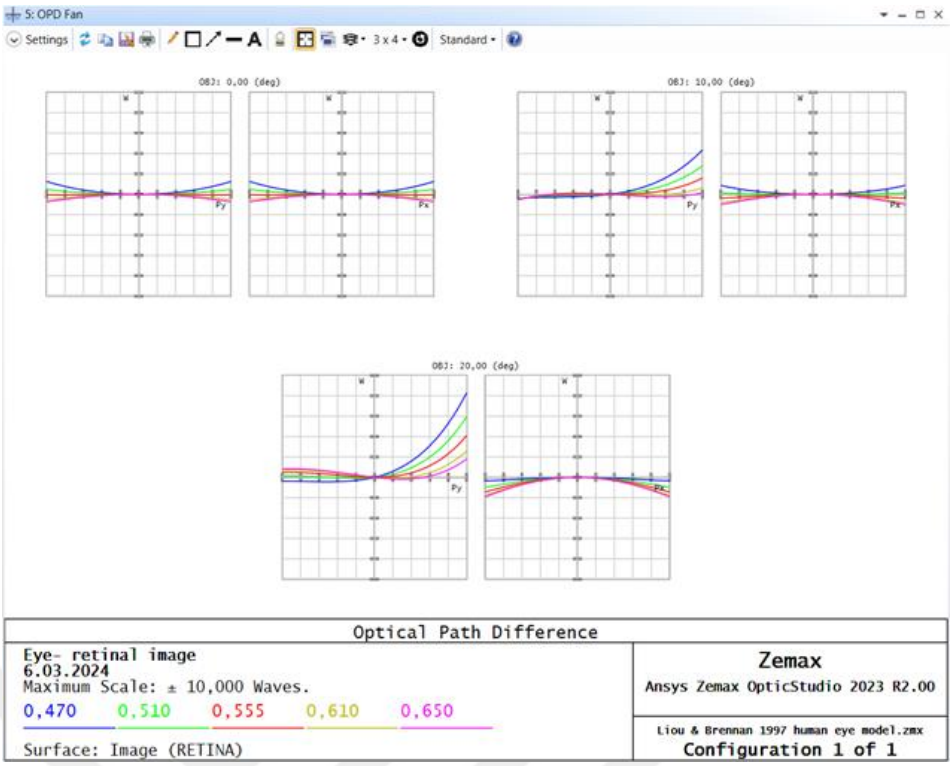

Figure 3.12 Zemax Optical Path Difference (OPD) fan of the human eye model with aspherical IOL design (for 3 different field and white light).

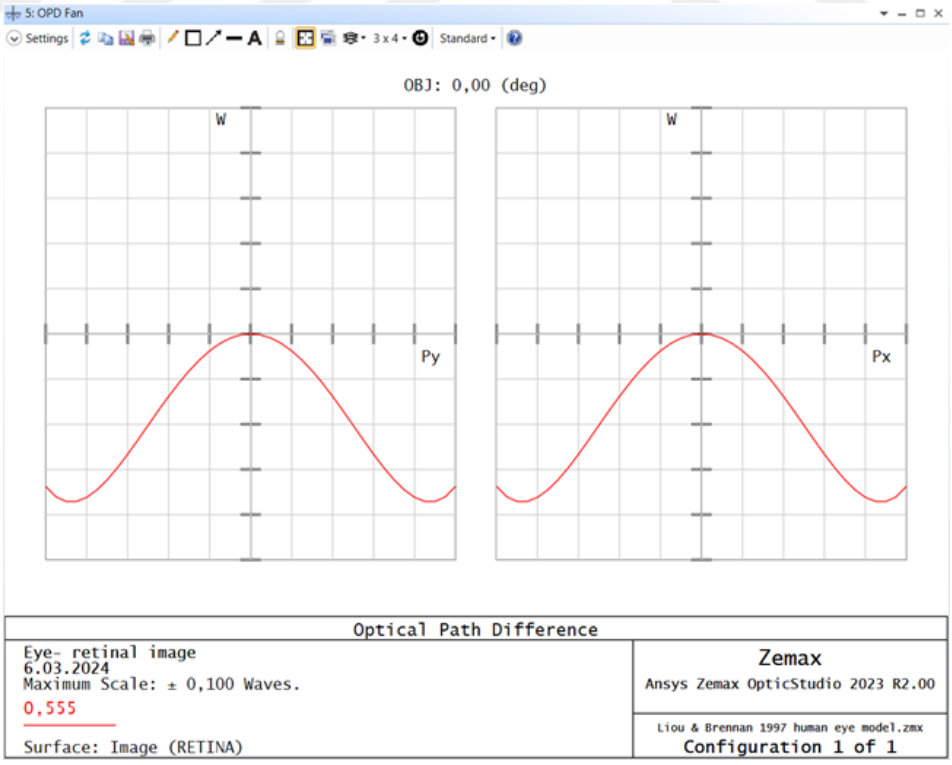

Figure 3.13 Zemax OPD fan of the human eye model with aspherical IOL design (for 0.555 μm wavelength).

An additional analysis tool that users may find useful during the IOL design process is Zemax's Extended Scene Analysis. The Geometric Bitmap Image Analysis feature creates an RGB color image based on ray tracing data using an RGB bitmap file as the source [32]. This feature is beneficial for various applications such as visualizing distortion or representing the appearance of displayed objects. The settings used for the analysis (Figure 3.14 and Figure 3.16), along with the results for the Alex (Figure 3.15) and USAF (Figure 3.17) images, are provided below.

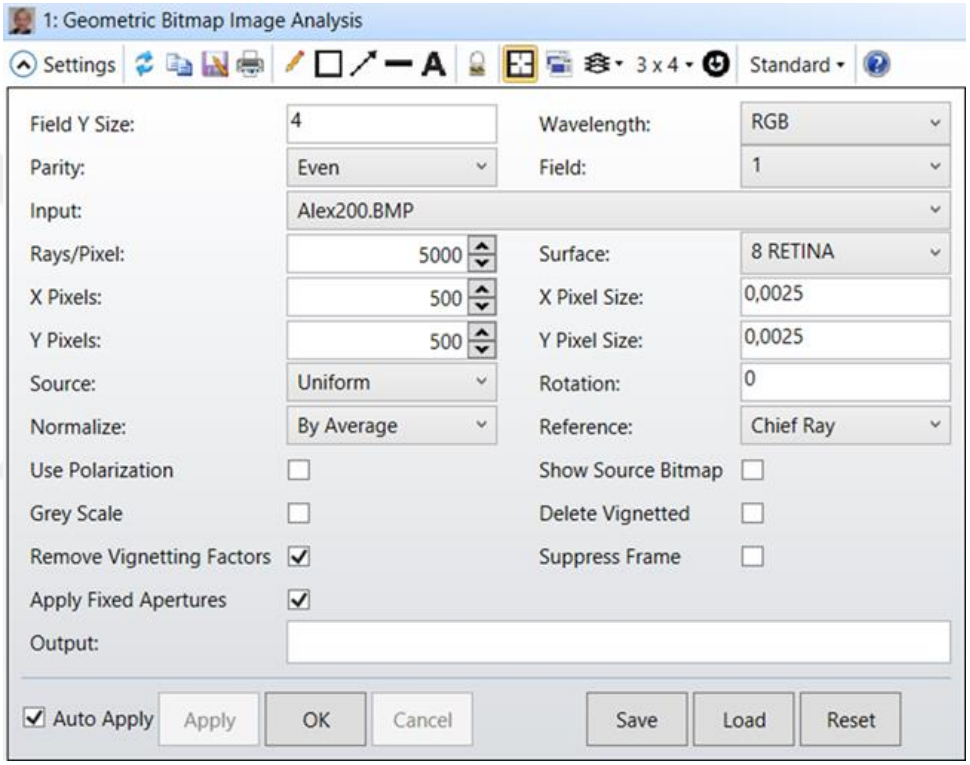

Figure 3.14 The setting used in Zemax image analysis (for Alex BMP).

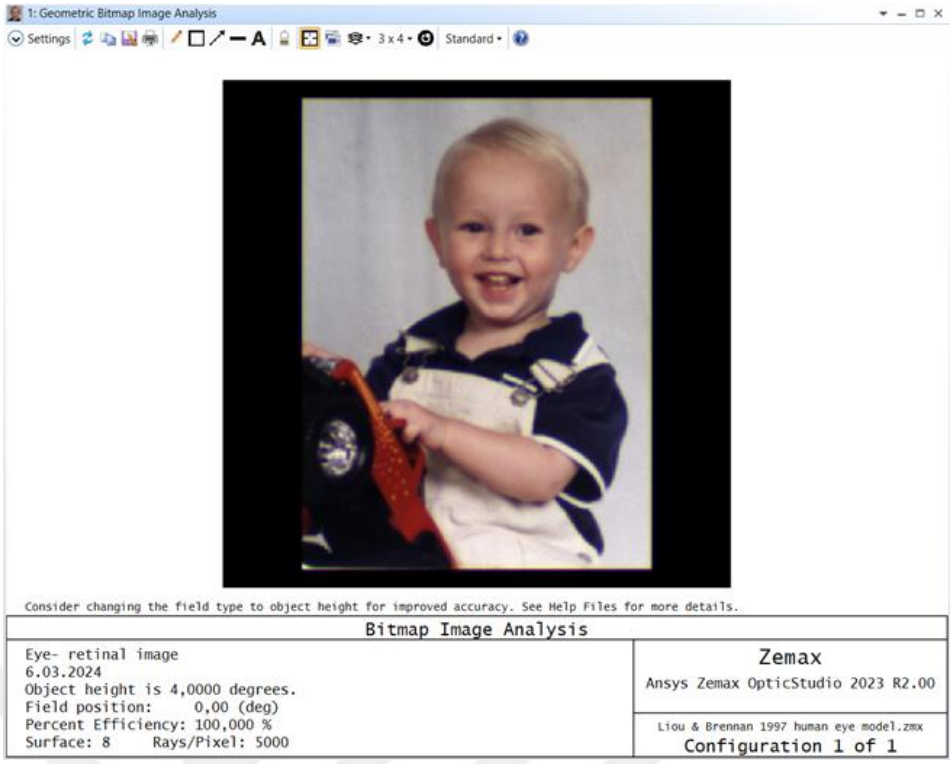

Figure 3.15 Zemax image analysis of the human eye model with aspherical IOL design (for Alex BMP).

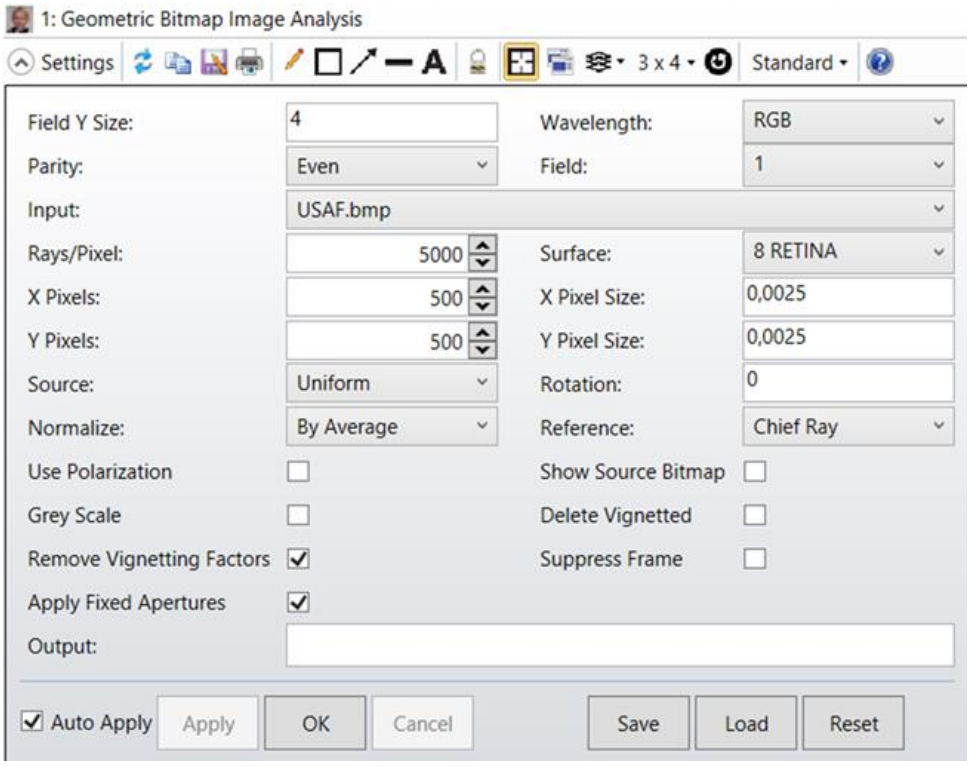

Figure 3.16 The setting used for Zemax image analysis (for USAF BMP).

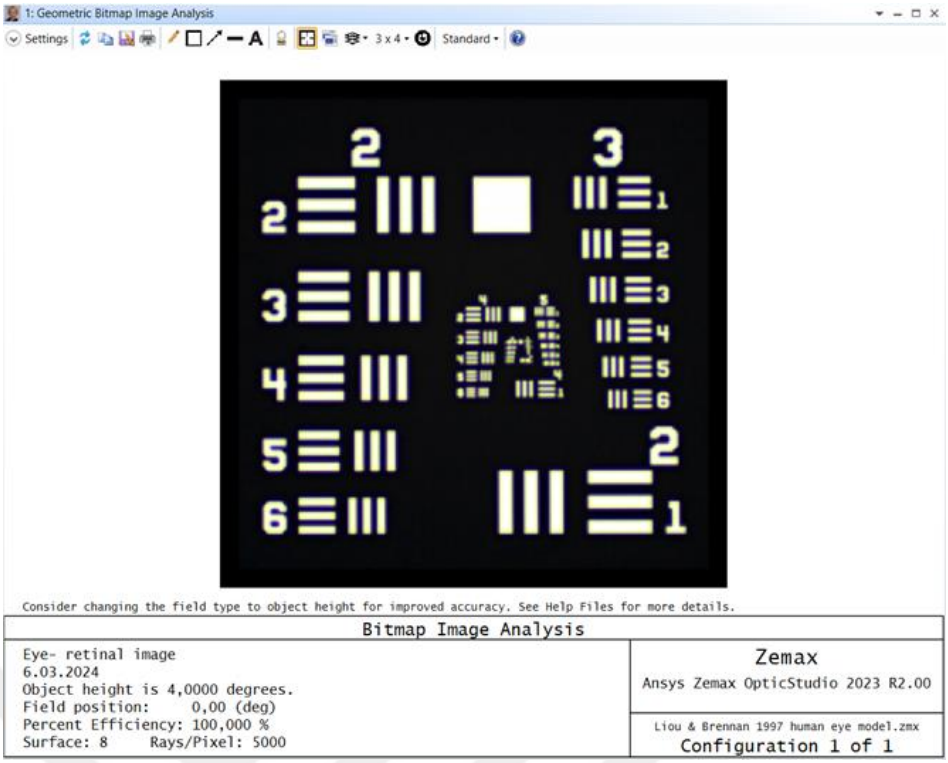

Figure 3.17 Zemax image analysis of the human eye model with aspherical IOL design (for USAF BMP).

3.2.3 ISO 11979-2 Model Eye 1 Design

In order to analyze the performance of the intraocular lens and evaluate its compliance with the standard, the designed aspherical IOL was included in the eye model given in the ISO 11979-2 standard [33]. In this study, Model Eye 1 defined in the ISO 11979-2 standard was used.

The characteristics of the Model Eye 1, as specified in the ISO 11979-2 standard, are as follows [42]:

- The Model Eye 1 features a cornea with minimal spherical aberration.
- The front surface of the IOL is positioned axially between 26 mm and 28 mm ahead of the focal point of the model cornea, with the refractive index of the medium of image space set at 1.336.
- The intraocular lens (IOL) is placed within a liquid medium situated between two flat windows.
- The image plane is located in the air, beyond the final window.

A potential implementation of Model Eye 1 is depicted in Figure 3.18 and detailed in Table 3.1. Numerous alternative implementations are feasible [42].

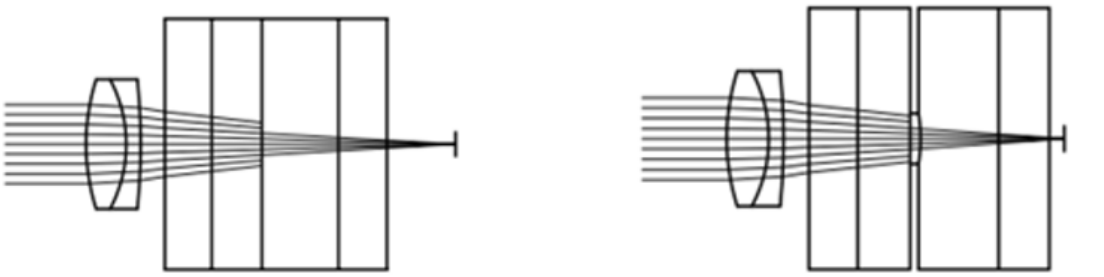

a) Without IOL b) With a 30D spherical IOL in place

Figure 3.18 Model eye 1 configuration [42].

Table 3.1 Description of a model eye 1 (with 3 mm aperture at surface 6) [42].

Surface number	Surface radius mm	Separation space mm	Diameter mm	Refractive index
1	24,590	5,21	16	1,620
2	- 15,580	1,72	16	1,694
3	- 90,200	3,0	16	1,000
4	∞	6,0	32	1,519
5	∞	6,25	32	1,336
6	∞	10,0	3,0	1,336
7	∞	6,0	32	1,519
8	∞	9,25	32	1,000
9	image plane (∞)			

If evaluated utilizing model eye 1, the modulation transfer function (MTF) of the model eye with the intraocular lens (IOL) configuration must be greater than or equal to 0.43 at a spatial frequency of 100 mm^{-1} [42].

According to the ISO standard for intraocular lenses, the primary wavelength is set to λ_0 = 546 nm [33]. The system's back focal length was optimized for the smallest RMS wavefront error through the utilization of the Quick Focus tool.

The Model Eye 1 specified in the ISO 11979-2 standard was simulated in the Zemax program, optical performance analyses were conducted for the designed aspheric lens. The simulation results from Zemax are as follows:

The Zemax sequential mode lens data of the ISO model eye 1 configuration with the aspheric IOL design are shown in Figure 3.19.

Lens Data

Update: All Windows

Surface 1 Properties

Configuration 1/1

	Surface Type		Comment	Radius	Thickness	Material	Coating	Clear Semi-Dia	Chip Zone	Mech Semi-Dia	Conic	TCE x 1E-6
0	OBJECT	Standard		Infinity	Infinity			0,000	0,000	0,000	0,000	0,000
1		Standard		Infinity	5,000			2,611	0,000	2,611	0,000	0,000
2	(aper)	Standard	Cornea	24,590	5,210	SSK4		8,000 U	0,000	8,000	0,000	-
3	(aper)	Standard		-15,580	1,720	SF8		8,000 U	0,000	8,000	0,000	-
4	(aper)	Standard		-90,200	3,000			8,000 U	0,000	8,000	0,000	0,000
5	(aper)	Standard		Infinity	6,000	BK7		16,000 U	0,000	16,000	0,000	-
6	(aper)	Standard	Aqueous	Infinity	6,250	1,33,0,0 M		16,000 U	0,000	16,000	0,000	0,000
7	STOP (aper)	Standard	Pupil	Infinity	0,000	1,33,0,0 P		1,500 U	0,000	1,500 U	0,000	0,000
8	(aper)	Standard	Lens	11,420	1,000	1,48,52,0 M		3,000 U	0,000	16,000	-0,270	0,000
9	(aper)	Standard	Aqueous	-19,480	9,000 T	1,33,0,0 P		3,000 U	0,000	3,000 U	-0,270	0,000
10	(aper)	Standard		Infinity	6,000	BK7		16,000 U	0,000	16,000	0,000	-
11		Standard		Infinity	3,250			0,335	0,000	16,000	0,000	0,000
12	IMAGE	Standard	Retina	Infinity	-			1,605E-03	0,000	1,605E-03	0,000	0,000

Figure 3.19 Zemax sequential mode lens data of the ISO model eye 1 configuration with the aspheric IOL design.

The Zemax layout of the ISO model eye 1 configuration with the aspheric IOL design is shown in Figure 3.20.

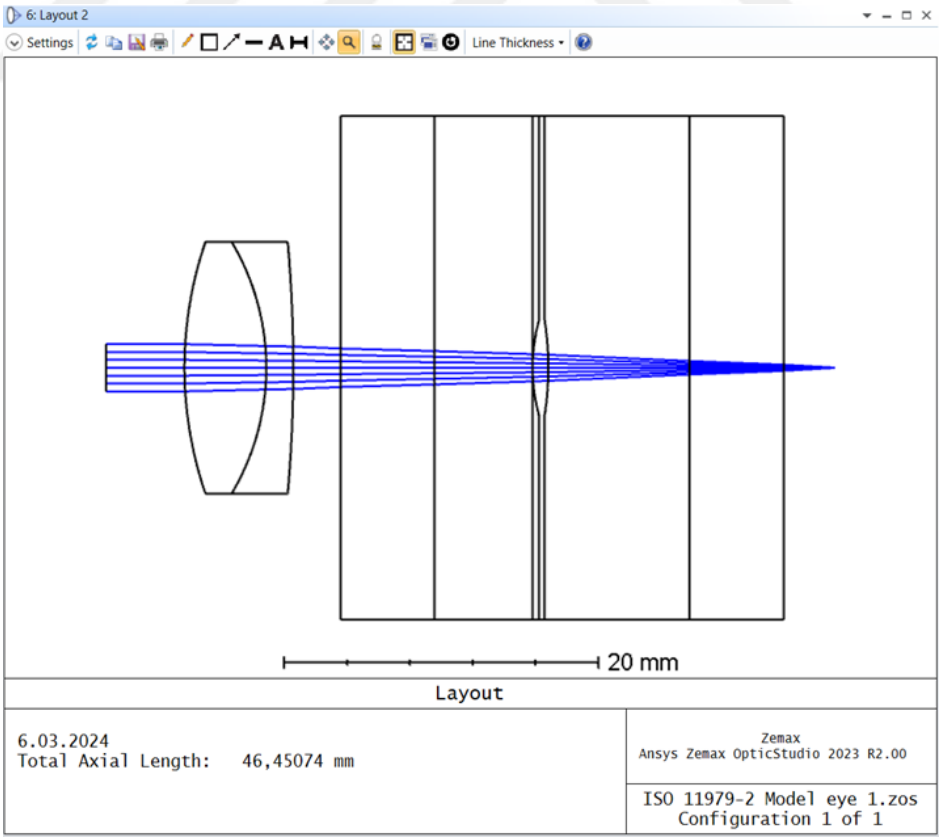

Figure 3.20 Zemax layout of the ISO model eye 1 configuration with the aspheric IOL design.

The Zemax MTF curve of the ISO model eye 1 configuration with the aspheric IOL design for a 0.546 μm wavelength is given in Figure 3.21. This graph indicates that the modulation transfer function (MTF) at a spatial frequency of 100 mm^{-1} is greater than 0.43, demonstrating the compliance of the designed lens with the ISO 11979-2 standard requirement.

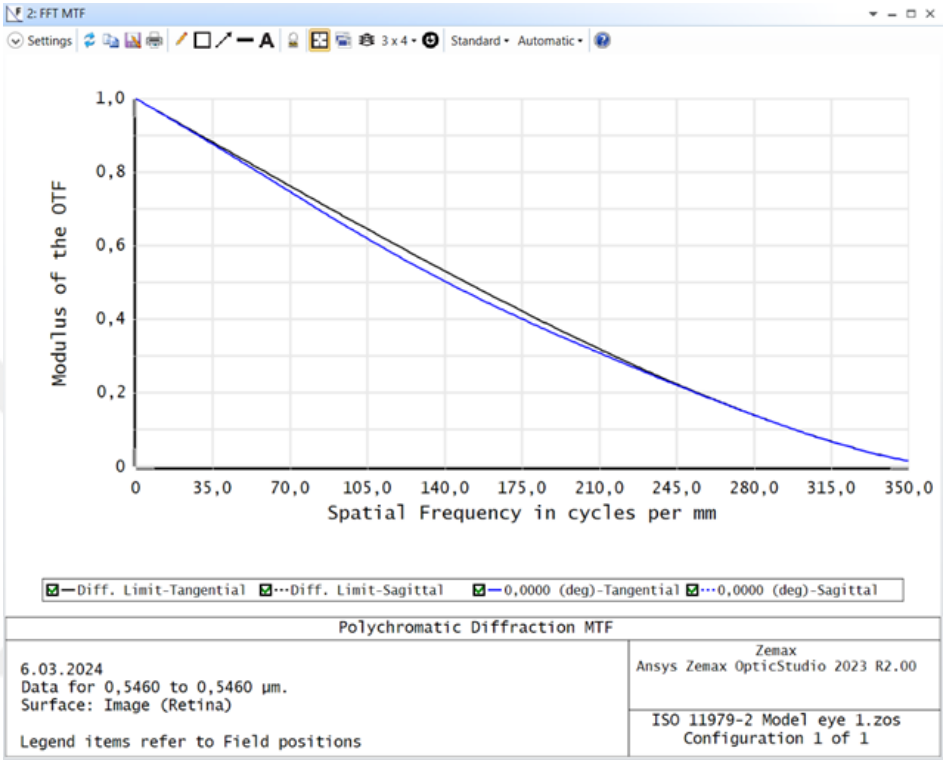

Figure 3.21 Zemax MTF curve of the ISO model eye 1 configuration with the aspheric IOL design.

Furthermore, the Zemax spot diagram of the ISO model eye 1 configuration with the aspheric IOL design for a 0.546 μm wavelength is shown in Figure 3.22, while the Zemax transverse ray fan plot is provided in Figure 3.23.

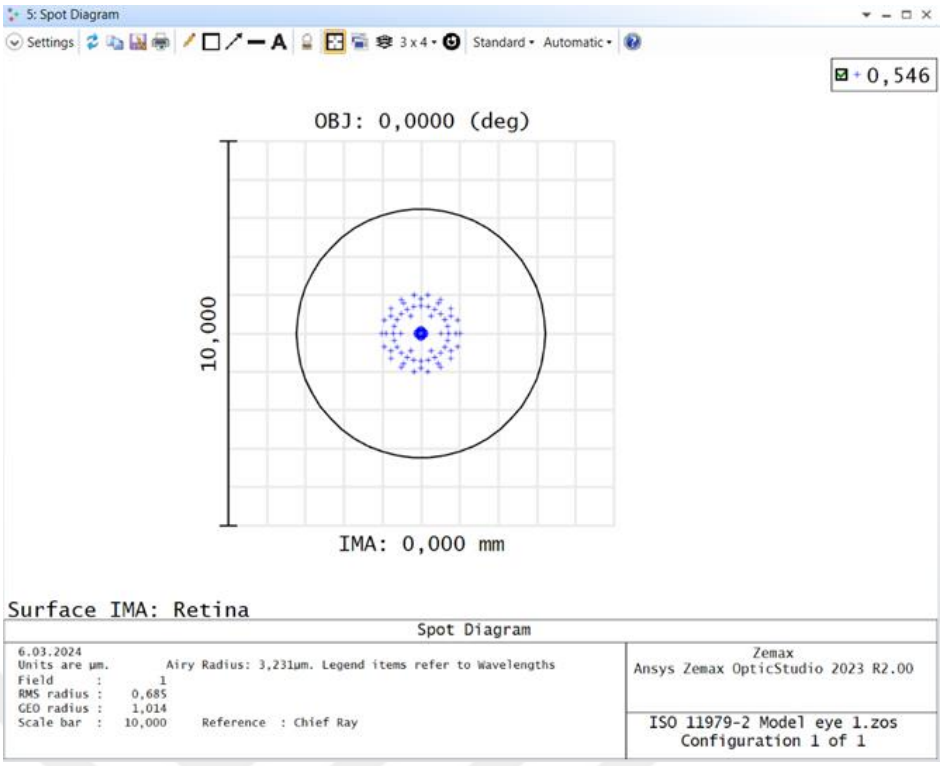

Figure 3.22 Zemax spot diagram of the ISO model eye 1 configuration with the aspheric IOL design.

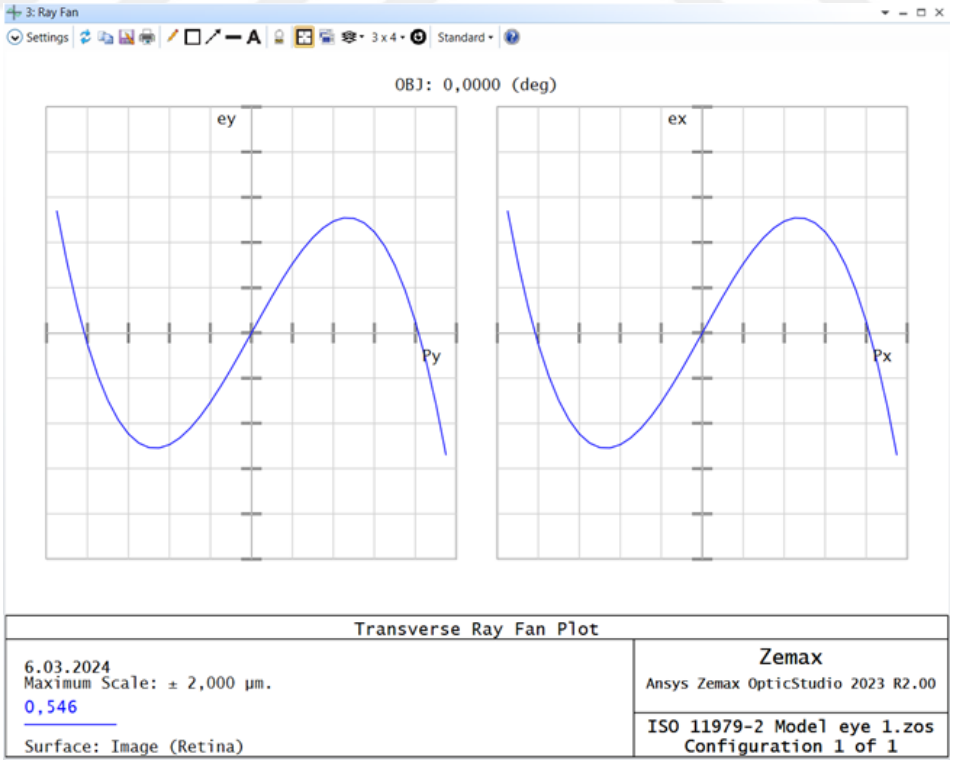

Figure 3.23 Zemax transverse ray fan plot of the ISO model eye 1 configuration with the aspheric IOL design.

Finally, the Zemax OPD fan of the ISO model eye 1 configuration with the aspheric IOL design for a 0.546 μm wavelength is given in Figure 3.24.

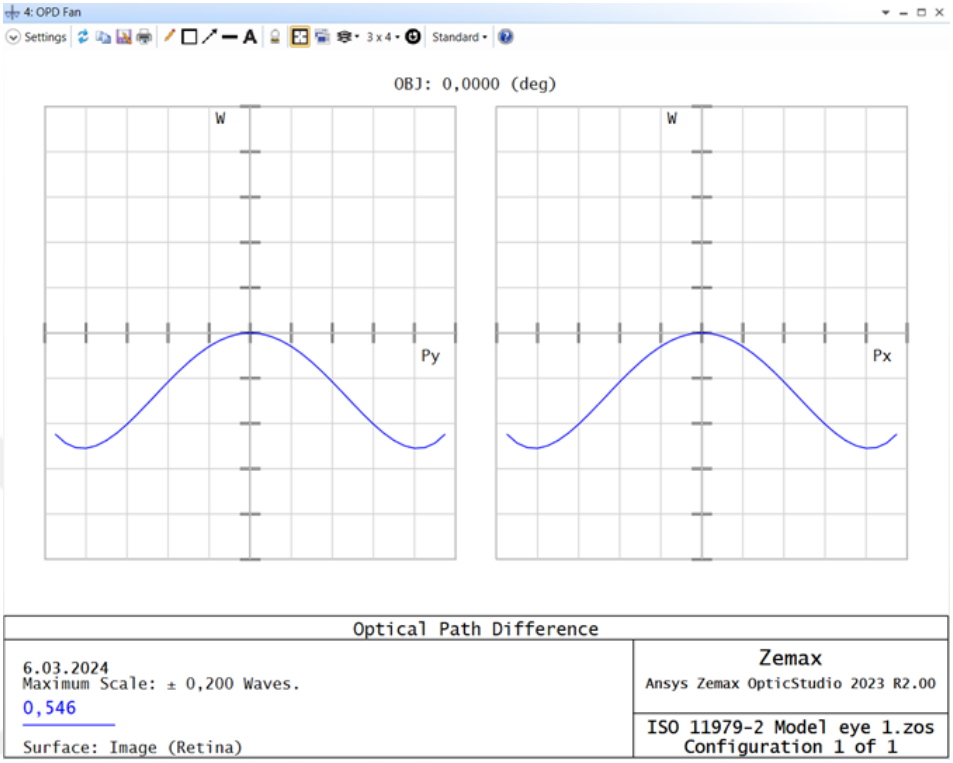

Figure 3.24 Zemax OPD fan of the ISO model eye 1 configuration with the aspheric IOL design.

CHAPTER 4
RESULT AND DISCUSSION

4.1 Design Verification and Optical Measurement Results

For design verification, four intraocular lenses (referred to as A, B, C, D), designed using different software program and manufactured for commercial purposes, were included in this study. To accomplish this, four intraocular lenses, each with different dioptric power and design (spherical and aspherical) and produced from different materials (hydrophilic and hydrophobic), were selected.

The characteristics of the intraocular lenses used in this study, referred to as A, B, C and D are as follows:

IOL A: This is a hydrophobic IOL with a power of +5.50 D, a monofocal and has a spherical design.

IOL B: This is a hydrophobic IOL with a power of +19.00 D, a monofocal and has a spherical design.

IOL C: This is a hydrophilic IOL with a power of +20.00 D, a monofocal and has an aspherical design.

IOL D: This is a hydrophilic IOL with a power of +22.00 D, a monofocal and has an aspherical design.

It should be emphasized here that all four types of lenses (A, B, C, D) have been successfully implanted for many years, contributing to high patient satisfaction. This has been evidenced by various clinical studies conducted in the past. The purpose of their inclusion in this study is not performance analysis, but rather design verification.

4.1.1 Comparison of Optical Measurement Results

These four intraocular lenses (IOLs), designated as A, B, C, and D, were simulated using both the 'Human Eye Model' and the 'ISO Eye Model' in the OpticStudio

Zemax program, and their MTF graphs were analyzed. Subsequently, MTF measurements were taken for these four lenses using the PMTF device by Lambda-X under cleanroom conditions. MTF measurements of the intraocular lenses were conducted under cleanroom conditions using a 546 nm wavelength and 3 mm aperture parameters, in accordance with the requirements of the ISO 11979-2 standard.

The optical performance of the IOLs was verified by comparing their modulation transfer functions. To ensure an accurate comparison, optical performance analyses in Zemax were performed using the same parameters (546 nm wavelength and 3 mm aperture) as utilized in the PMTF device.

When comparing the Zemax simulation results with the measurement results obtained from the PMTF device, it was observed that the optical performance analyzes gave very close and consistent results.

The measurement results and comparative MTF graphs for the four different lenses are presented in the Figures 4.1 to Figure 4.4. The similarity of the results is quite striking.

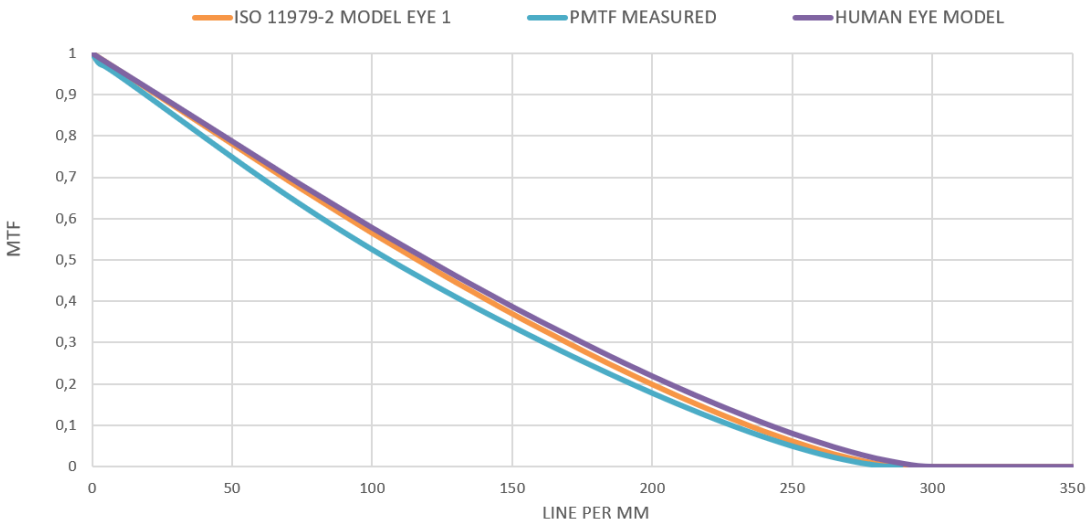

Figure 4.1 The comparative MTF graph of IOL A.

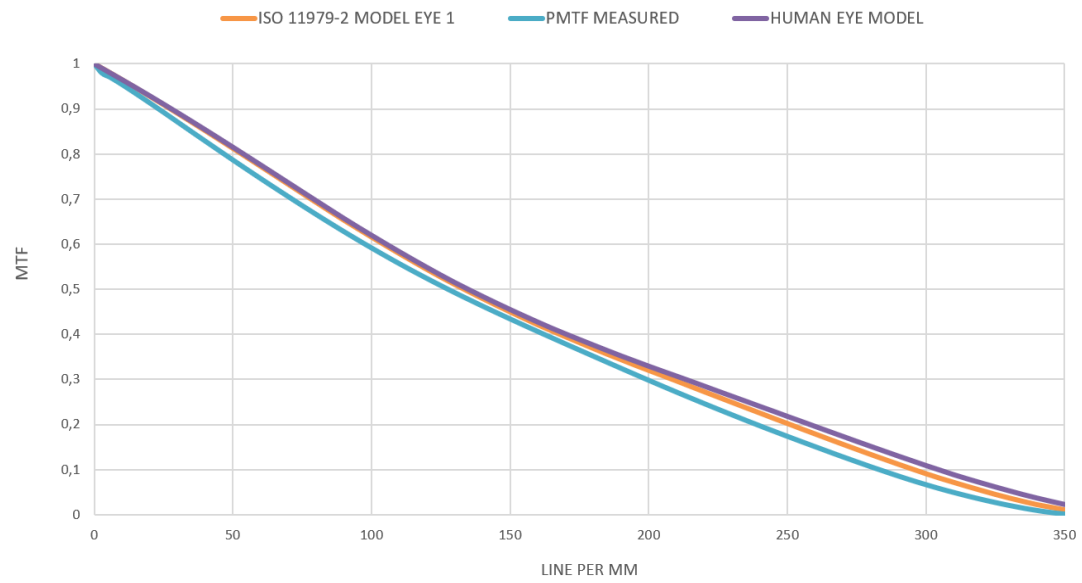

Figure 4.2 The comparative MTF graph of IOL B.

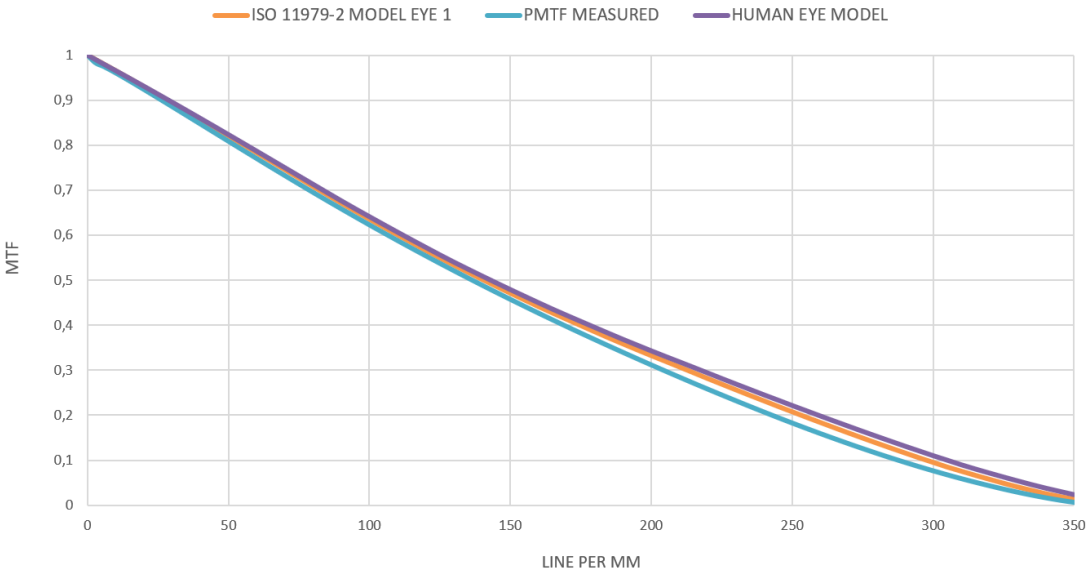

Figure 4.3 The comparative MTF graph of IOL C.

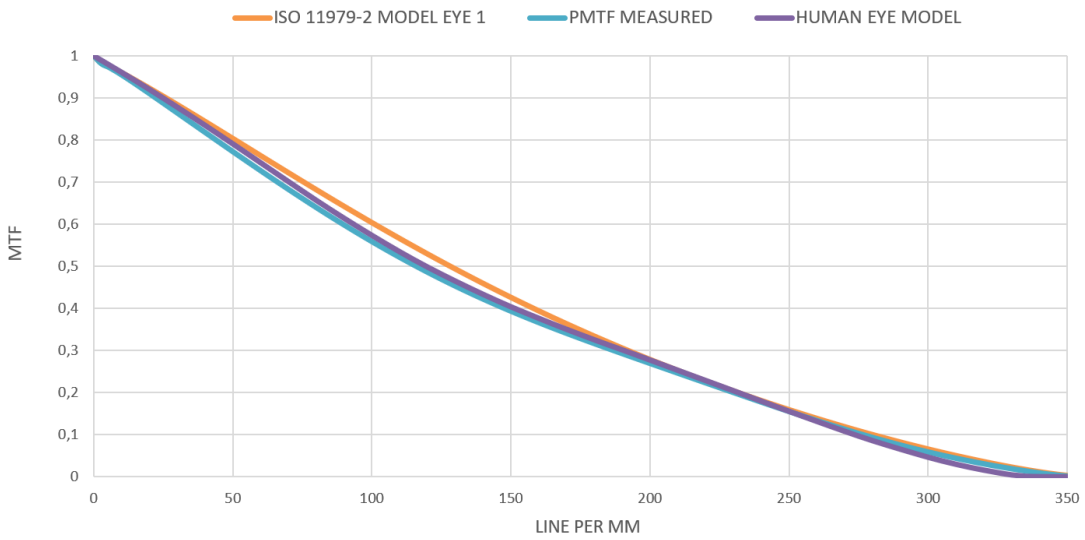

Figure 4.4 The comparative MTF graph of IOL D.

CHAPTER 5
CONCLUSIONS

In this thesis, an aspheric intraocular lens with negative spherical aberration, which compensates for the positive spherical aberration of the cornea, has been designed using the Zemax OpticStudio program. Initially, the simplified human eye model based on the literature was created in Zemax program. Following this, an aspheric intraocular lens was designed based on this eye model. The optical performance of the designed intraocular lens was analyzed by incorporating it into the ISO Model Eye 1 model defined in the ISO 11979-2 standard. Four intraocular lenses designed using different software programs and produced for commercial purposes were simulated using ISO Model Eye 1 and Human Eye Models in the Zemax program, and then Modulation Transfer Function (MTF) analyzes were performed. Subsequently, MTF measurements were obtained for these four lenses using the PMTF device under clean room conditions. Finally, the design was validated by comparing the results of Zemax simulation with those obtained from the PMTF device. Optical quality assessments were conducted using parameters of a 3.0 mm aperture size and a wavelength of 546 nm. The comparison of the Zemax simulation results with the measurements from the PMTF device revealed very close and consistent results in optical performance analyses.

In conclusion, it is inferred that the design and optical performance analyses of intraocular lenses can be successfully accomplished using the tolerance and programming features of Zemax OpticStudio software. This methodology can used as a reliable tool for intraocular lens manufacturers in the industry to evaluate and optimize design parameters.

REFERENCES

[1] Wikipedia contributors, "Cataract surgery," 30 June 2024. [Online]. Available: https://en.wikipedia.org/w/index.php?title=Cataract_surgery&oldid=1231837998.

[2] S. Abacıoğlu, "Katarakt Cerrahisi Yapılacak Hastalarda 1. ve 2. Göz Cerrahileri Öncesi, Hastaların Endişe Düzeylerinin Araştırılması," Afyon Kocatepe Üniversitesi Sağlık Bilimleri Enstitüsü, Afyon, 2009.

[3] Ö. Dr. Önal, "Katarakt Cerrahisinde Kullanılan Torik Göziçi Lenslerin Astigmatik Düzeltici Etkisi ve Hastaların Yaşam Kalitesi Üzerine Olan Etkilerinin Değerlendirilmesi," Eskişehir Osmangazi Üniversitesi Tıp Fakültesi, Eskişehir, 2017.

[4] M. T. Sheehan, "Eye modelling for personalised intraocular lens design," National University of Ireland, Science Faculty, Galway, 2012.

[5] Türk Oftalmoloji Derneği, Optik Refraksiyon Rehabilitasyon Temel Bilgiler, İstanbul: Türk Oftalmoloji Derneği Eğitim Yayınları, 2010.

[6] İ. Çevik, H. Çakmak, Ö. Çelik and P. Okyay, "Yaşam boyu göz sağlığı: “2020 vizyonu: görme hakkı”," *ESTÜDAM Halk Sağlığı Dergisi,* vol. 6, no. 3, 2021.

[7] "Eye Care Professionals," n.d. [Online]. Available: https://renoeyecare.com/blog/eye-care-professionals/light-adjustable-lenses/.

[8] J. Schwiegerling, "Intraocular Lenses," in *Handbook of Optics*, 2010, pp. 3,21-11.

[9] Wikimedia Commons, 13 Şubat 2024. [Online]. Available: https://commons.wikimedia.org/w/index.php?title=File:Cataracts.png&oldid=8

51365334.

[10] E. Dr. Erden, "Trifokal Göziçi Lens İmplantasyonu Sonuçlarımız," Dokuz Eylül Üniversitesi Tıp Fakültesi, İzmir, 2019.

[11] E. Dr. Ergül, "Lens Gücünün Yeni Biometri Formülleri Kullanılarak Hesaplanması," İstanbul Üniversitesi İstanbul Tıp Fakültesi, İstanbul, 2021.

[12] Wikipedia contributors, "Phacoemulsification," 9 May 2024. [Online]. Available: https://en.wikipedia.org/wiki/Phacoemulsification.

[13] "Shinagawa Lasik & Aesthetics," n.d. [Online]. Available: https://shinagawa.ph/eye-services/what-is-cataract/laser-assisted-cataract/.

[14] Wikipedia contributors, "Intraocular Lens," 9 June 2024. [Online]. Available: https://en.wikipedia.org/wiki/Intraocular_lens.

[15] M. Yanoff and J. S. Duker, Ophthalmology, Elsevier Health Sciences, 2018.

[16] T. Ö. Dr. Öğr. Üyesi YAŞAR and İ. N. Çınar, Katarakt Cerrahisi ve İntraoküler Lensler, Ankara: Iksad Publications, 2023.

[17] D. J. Apple and J. Sims , "Harold Ridley and the invention of the intraocular lens," *Survey of ophthalmology*, vol. 40, no. 4, pp. 279-292, 1996.

[18] S. Shah and Y. Shah, Implants in ophthalmology, New Delhi: All India Ophthalmological Society, 2008.

[19] S. Čanović, S. Konjevoda, A. Didović Pavičić and R. Stanić, Intraocular Lens (IOL) Materials, 2020.

[20] B. Horizonte, *Lens Design with Orthogonal Sinusoidal Pattern and Focal-Range Classification Algorithm.*, Universidade Federal de Minas Gerais., 2020.

[21] R. E. Fischer, B. Tadic-Galeb and P. R. Yoder, Optical System Design, New

York: McGraw-Hill, 2000.

[22] Y. Kikuchi, "What Is the Modulation Transfer Function?," n.d.. [Online]. Available: https://www.olympus-lifescience.com/en/resources/white-papers/what-is-the-modulation-transfer-function/.

[23] R. Rawer, W. Stork, C. W. Spraul and C. Lingenfelder, "Imaging quality of intraocular lenses," *Journal of Cataract & Refractive Surgery,* vol. 31, no. 8, pp. 1618-1631, 31 August 2005.

[24] V. Argueta, "Mastering Spot Diagrams: Analyzing Optical System Quality," n.d. [Online]. Available: https://www.opticsforhire.com/blog/interpreting-spot-diagrams/.

[25] J. Laatikainen, "Design of Apochromatic Lenses," University of Eastern Finland, Physics, Kuopio, 2020.

[26] J. A. Shaw, "Wave-Front Aberrations," Montana State University, n.d.

[27] A. Riera Salva, "Design of refractive optical lenses for an infrared camera. (Unpublished master's thesis)," University of Liège, Liège, 2018.

[28] P. Gyulai, "How to understand OPD diagrams," n.d. [Online]. Available: https://cfftelescopes.eu/opd-diagrams-explained.

[29] M. S. d. Almeida and L. A. Carvalho, "Different Schematic Eyes and their Accuracy to the in vivo Eye: A Quantitative Comparison Study," *Brazilian Journal of Physics,* vol. 37, pp. 378-387, 2007.

[30] M. Tocci, "How to model the human eye in OpticStudio," Search the Zemax Knowledgebase, 31 March 2021. [Online]. Available: https://support.zemax.com/hc/en-us/articles/1500005575002-How-to-model-the-human-eye-in-OpticStudio.

[31] R. Watkins, "OpticStudio models of the human eye," Director of Strategic Development Optometry and Vision Science, Flinders University, 31 March

2021. [Online]. Available: https://support.zemax.com/hc/en-us/articles/1500005575082-OpticStudio-models-of-the-human-eye.

[32] J. E. Hernandez, "Using diffractive surfaces to model intraocular lenses," Using diffractive surfaces to model intraocular lenses, 2021.

[33] C. Timar-Fulep, "Realistic modeling of relief-type diffractive intraocular lenses using User-Defined Surface DLLs," 14 July 2022. [Online]. Available: https://support.zemax.com/hc/en-us/articles/7772225130259-Realistic-modeling-of-relief-type-diffractive-intraocular-lenses-using-User-Defined-Surface-DLLs.

[34] J. Pérez-Gracia, A. Varea, J. Ares, J. A. Vallés and L. Remón, "Evaluation of the optical performance for aspheric intraocular lenses in relation with tilt and decenter errors.," *PloS one*, vol. 15, no. 5, 2020.

[35] T. Eppig, K. Scholz, A. Löffler, A. Messner and A. Langenbucher, "Effect of decentration and tilt on the image quality of aspheric intraocular lens designs in a model eye.," *Journal of Cataract & Refractive Surgery,* vol. 35, no. 6, pp. 1091-1100, 2009.

[36] R. Montés-Micó, T. Ferrer-Blasco and A. Cerviño, "Analysis of the possible benefits of aspheric intraocular lenses: review of the literature.," *Journal of Cataract & Refractive Surgery,* vol. 35, no. 1, pp. 172-181, 2009.

[37] A. F. Borkenstein, E. M. Borkenstein, H. Luedtke and R. Schmid, "Impact of decentration and tilt on spherical, aberration correcting, and specific aspherical intraocular lenses: an optical bench analysis.," *Ophthalmic Research,* vol. 65, no. 4, pp. 425-436, 2022.

[38] Lambda-X, "PMTF," 2024. [Online]. Available: https://ophthalmics.lambda-x.com/pmtf/.

[39] W. contributors, "Lens," Wikipedia, The Free Encyclopedia, 15 June 2024. [Online]. Available:

https://en.wikipedia.org/w/index.php?title=Lens&oldid=1229176145.

[40] U. Sridhar and . K. Tripathy, Monofocal Intraocular Lenses, Treasure Island: StatPearls Publishing, 2022.

[41] S. Dewey, "Understanding Intraocular Lenses: The Basics of Design and Material," vol. 33, Focal Points, 2015.

[42] BS EN ISO 11979-2, *Ophthalmic implants - Intraocular lenses - Part 2: Optical properties and test methods,* Brussels: BSI Standards Publication, 2014.

APPENDIX A

SIMULATION RESULTS FOR TILT

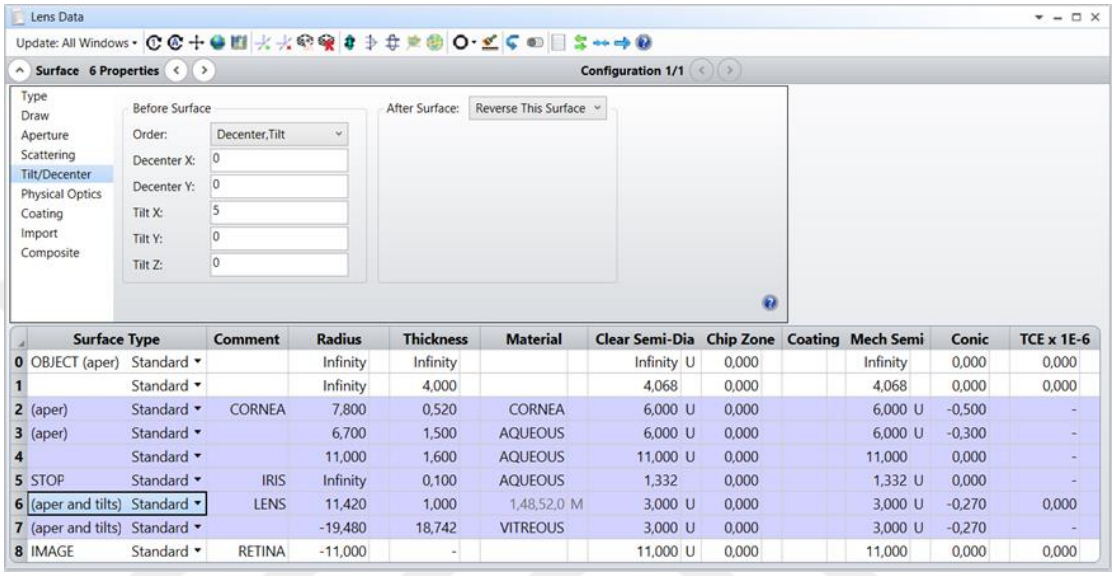

	Surface Type		Comment	Radius	Thickness	Material	Clear Semi-Dia	Chip Zone	Coating	Mech Semi	Conic	TCE x 1E-6
0	OBJECT (aper)	Standard		Infinity	Infinity		Infinity U	0,000		Infinity	0,000	0,000
1		Standard		Infinity	4,000		4,068	0,000		4,068	0,000	0,000
2	(aper)	Standard	CORNEA	7,800	0,520	CORNEA	6,000 U	0,000		6,000 U	-0,500	-
3	(aper)	Standard		6,700	1,500	AQUEOUS	6,000 U	0,000		6,000 U	-0,300	-
4		Standard		11,000	1,600	AQUEOUS	11,000 U	0,000		11,000	0,000	-
5	STOP	Standard	IRIS	Infinity	0,100	AQUEOUS	1,332	0,000		1,332 U	0,000	-
6	(aper and tilts)	Standard	LENS	11,420	1,000	1,48,52,0 M	3,000 U	0,000		3,000 U	-0,270	0,000
7	(aper and tilts)	Standard		-19,480	18,742	VITREOUS	3,000 U	0,000		3,000 U	-0,270	-
8	IMAGE	Standard	RETINA	-11,000	-		11,000 U	0,000		11,000	0,000	0,000

Figure A. 1 Zemax simulation lens data of the aspherical IOL design on the human eye model for 5° tilt.

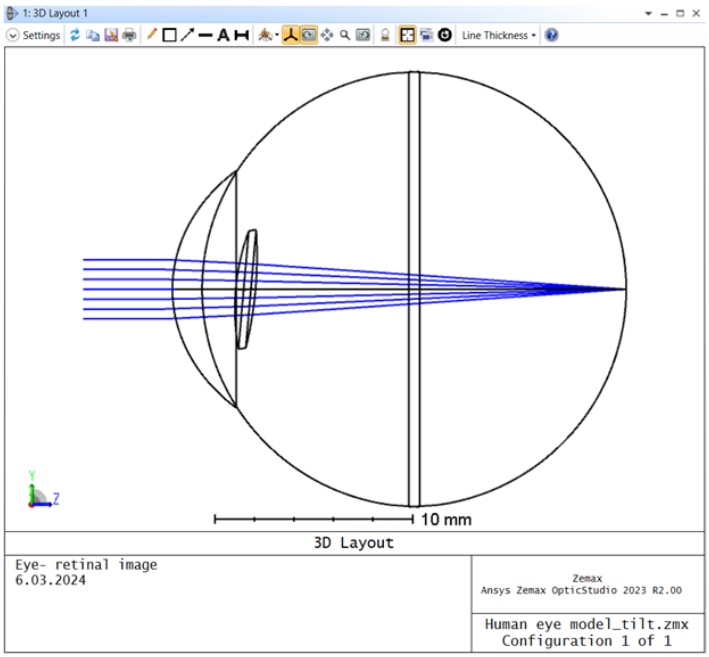

Figure A. 2 Zemax simulation 3D layout of the aspherical IOL design on the human eye model for 5° tilt.

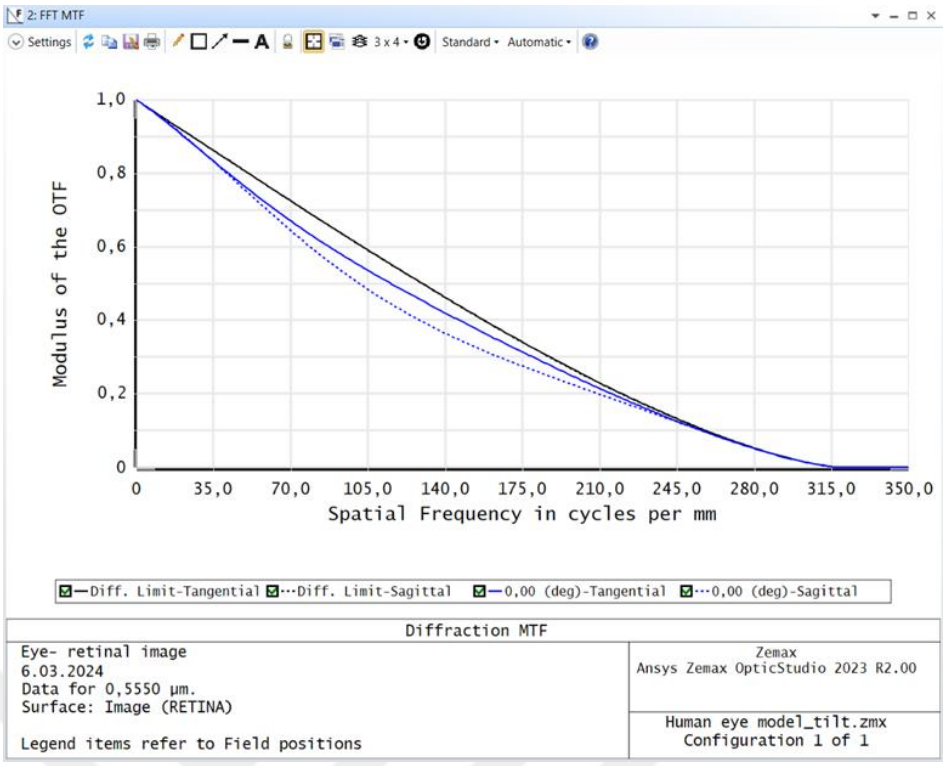

Figure A. 3 Zemax simulation MTF graph of the aspherical IOL design on the human eye model for 5° tilt.

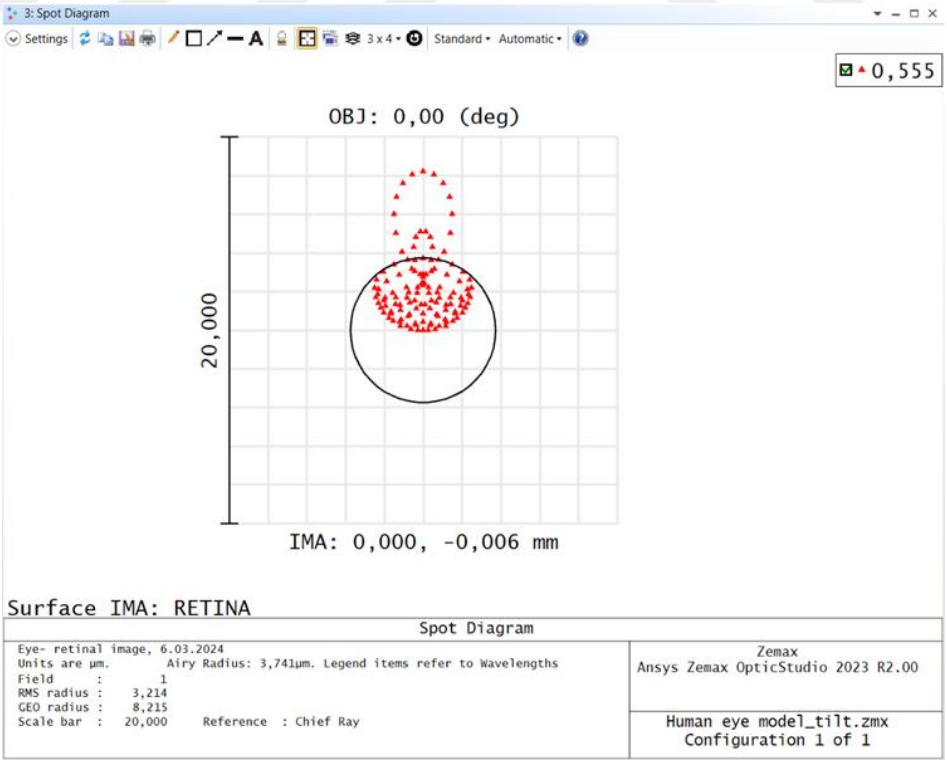

Figure A. 4 Zemax simulation spot diagram of the aspherical IOL design on the human eye model for 5° tilt.

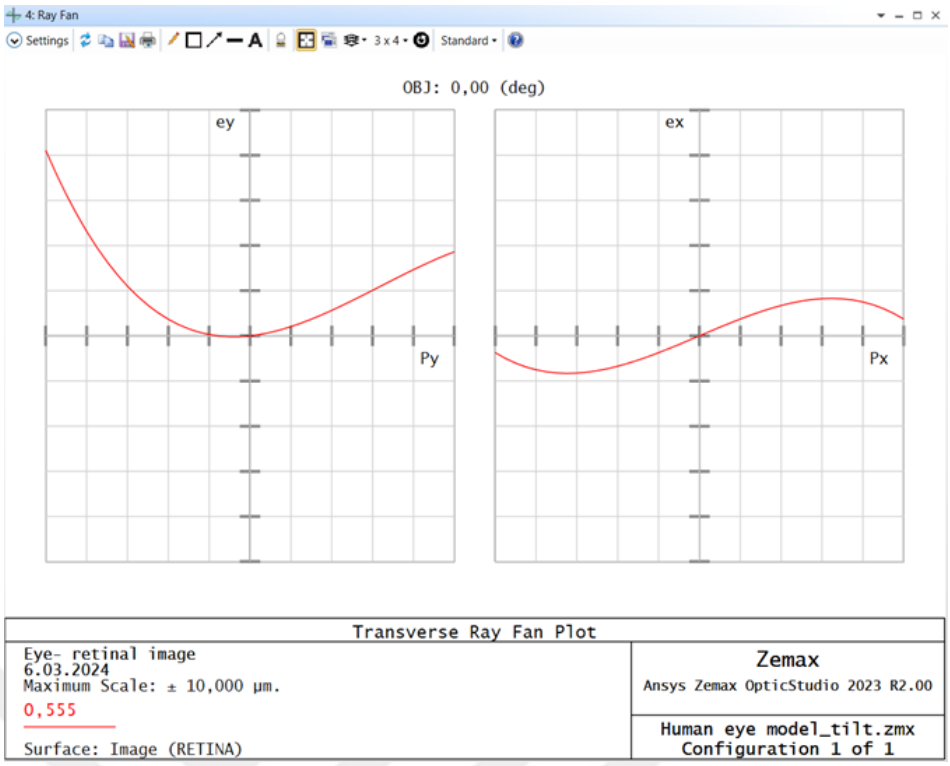

Figure A. 5 Zemax simulation ray fan of the aspherical IOL design on the human eye model for 5° tilt.

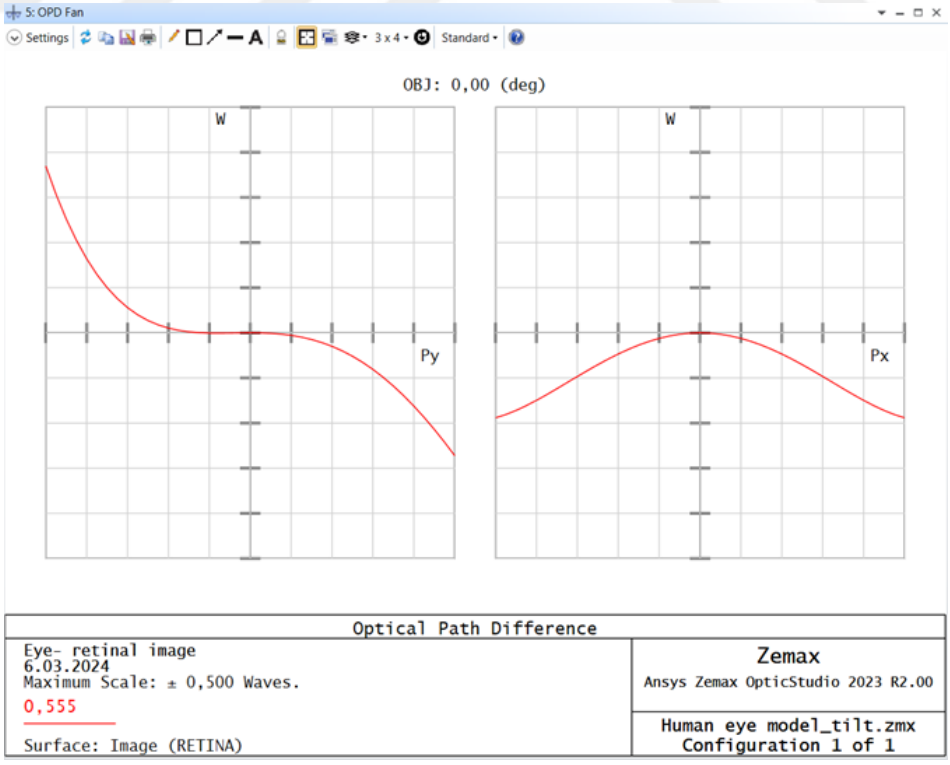

Figure A. 6 Zemax simulation OPD fan of the aspherical IOL design on the human eye model for 5° tilt.

APPENDIX B

SIMULATION RESULTS FOR DECENTRATION

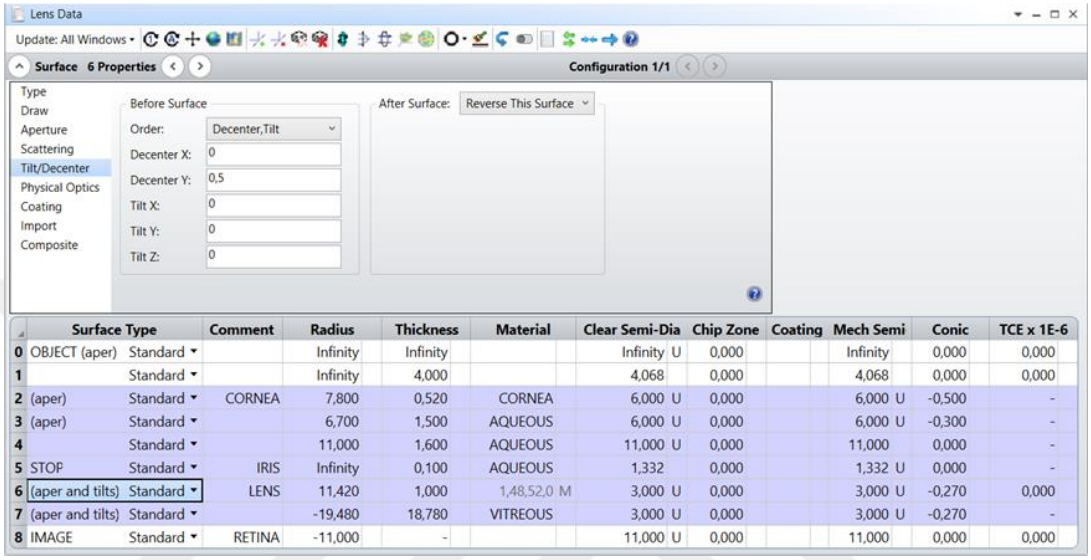

	Surface Type		Comment	Radius	Thickness	Material	Clear Semi-Dia	Chip Zone	Coating	Mech Semi	Conic	TCE x 1E-6
0	OBJECT (aper)	Standard		Infinity	Infinity		Infinity U	0,000		Infinity	0,000	0,000
1		Standard		Infinity	4,000		4,068	0,000		4,068	0,000	0,000
2	(aper)	Standard	CORNEA	7,800	0,520	CORNEA	6,000 U	0,000		6,000 U	-0,500	-
3	(aper)	Standard		6,700	1,500	AQUEOUS	6,000 U	0,000		6,000 U	-0,300	-
4		Standard		11,000	1,600	AQUEOUS	11,000 U	0,000		11,000	0,000	-
5	STOP	Standard	IRIS	Infinity	0,100	AQUEOUS	1,332	0,000		1,332 U	0,000	-
6	(aper and tilts)	Standard	LENS	11,420	1,000	1,48,52,0 M	3,000 U	0,000		3,000 U	-0,270	0,000
7	(aper and tilts)	Standard		-19,480	18,780	VITREOUS	3,000 U	0,000		3,000 U	-0,270	-
8	IMAGE	Standard	RETINA	-11,000	-		11,000 U	0,000		11,000	0,000	0,000

Figure B. 1 Zemax simulation lens data of the aspherical IOL design on the human eye model for 0.5 decentration.

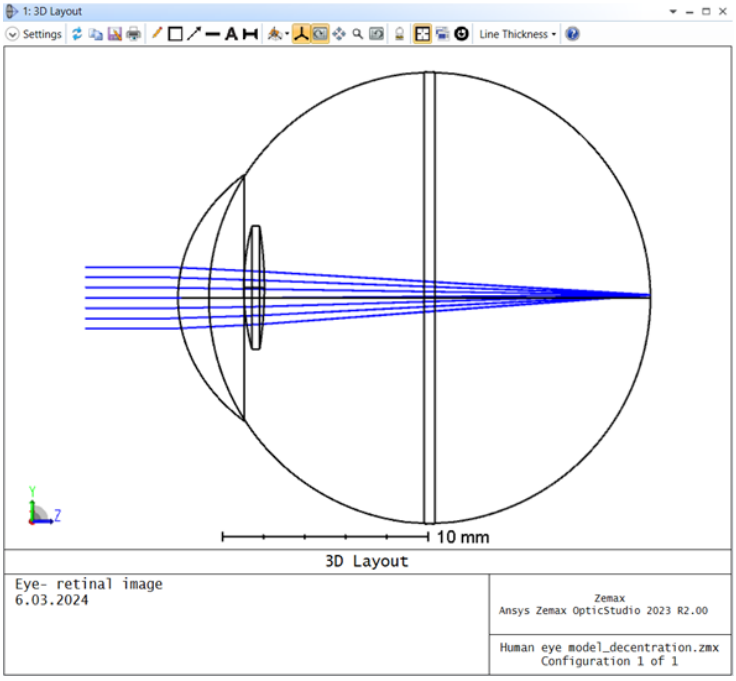

Figure B. 2 Zemax simulation 3D layout of the aspherical IOL design on the human eye model for 0.5 decentration.

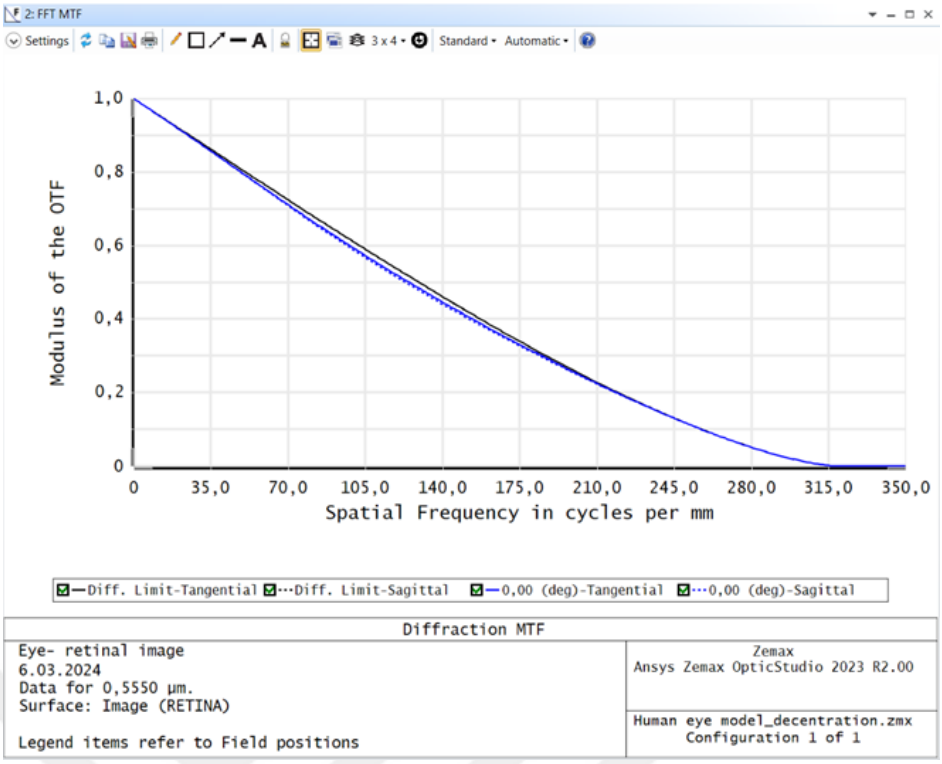

Figure B. 3 Zemax simulation MTF graph of the aspherical IOL design on the human eye model for 0.5 decentration.

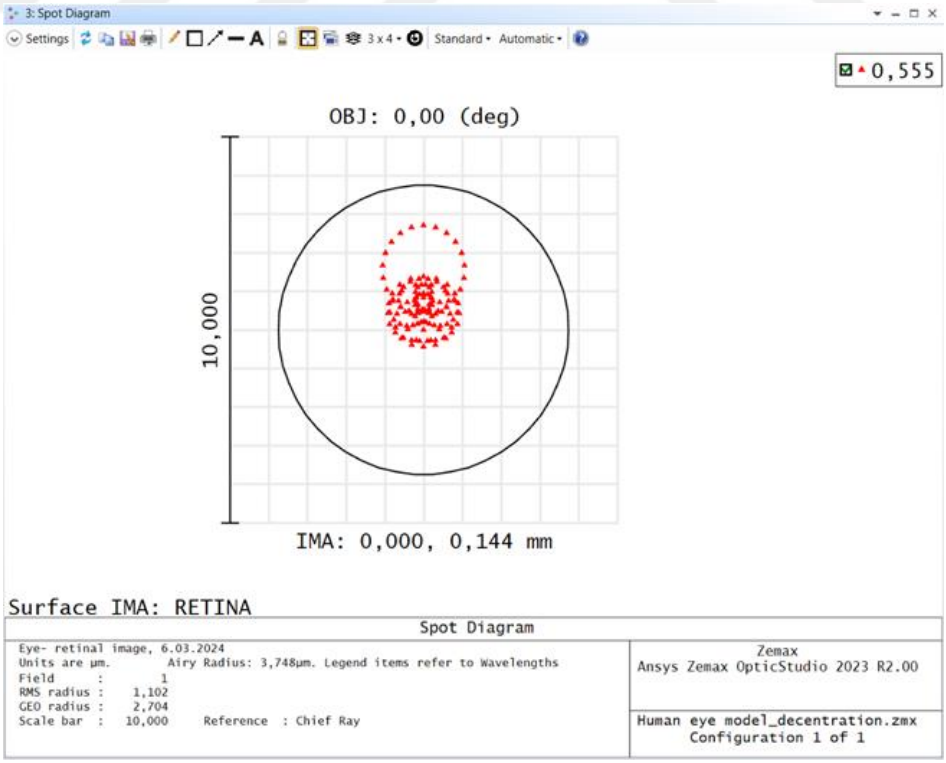

Figure B. 4 Zemax simulation spot diagram of the aspherical IOL design on the human eye model for 0.5 decentration.

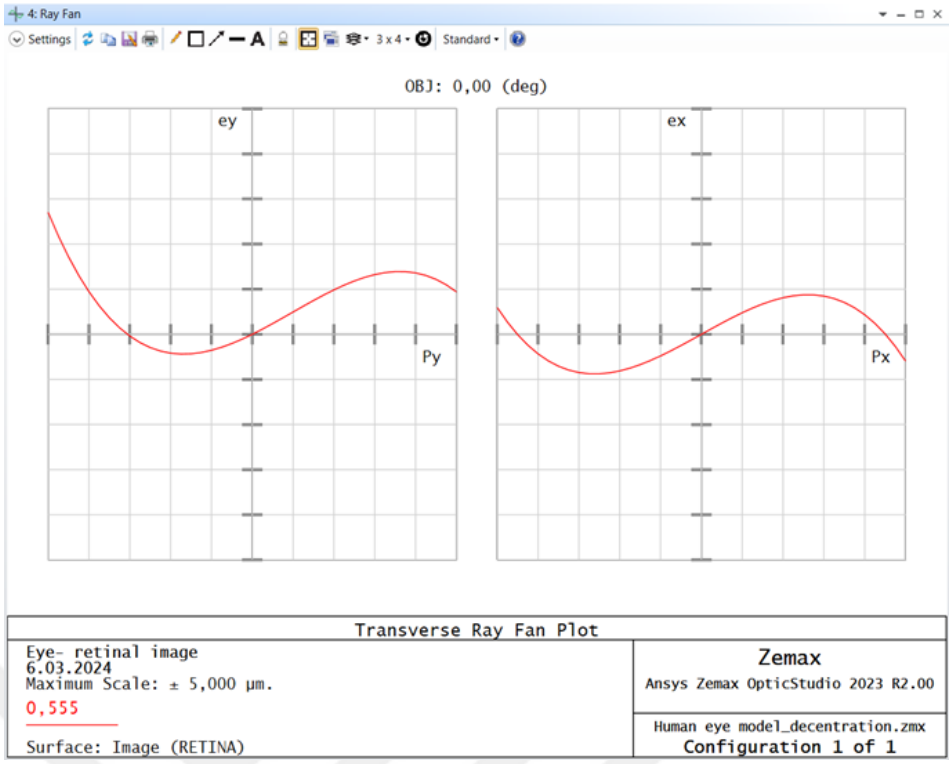

Figure B. 5 Zemax simulation ray fan of the aspherical IOL design on the human eye model for 0.5 decentration.

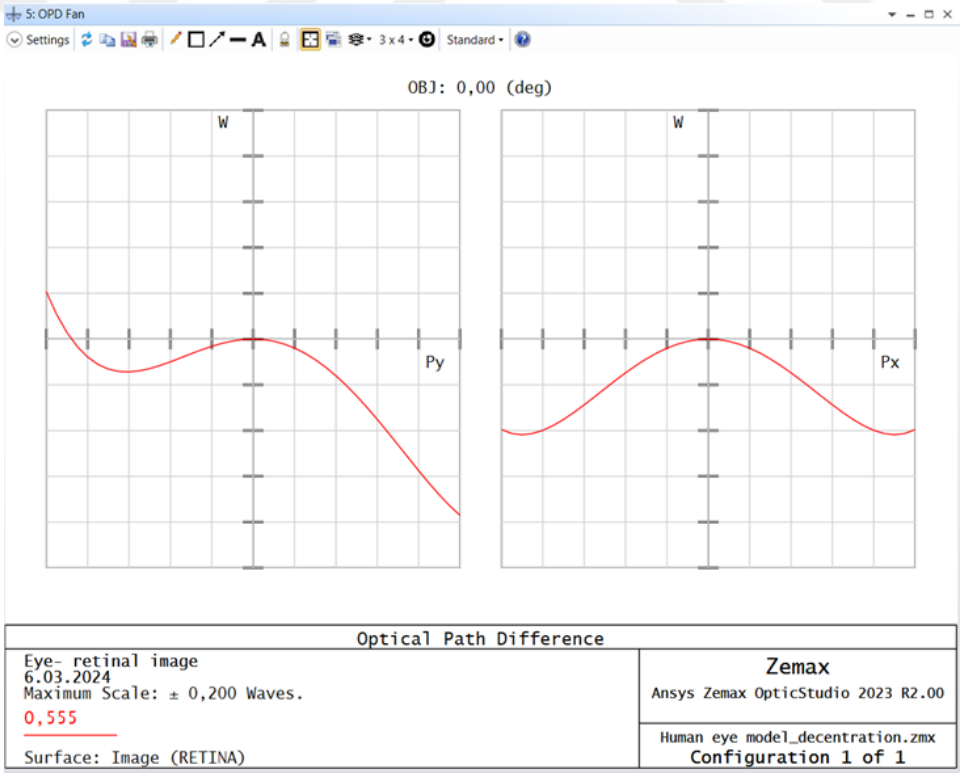

Figure B. 6 Zemax simulation OPD fan of the aspherical IOL design on the human eye model for 0.5 decentration.

APPENDIX C

SIMULATION RESULTS FOR TILT AND DECENTRATION

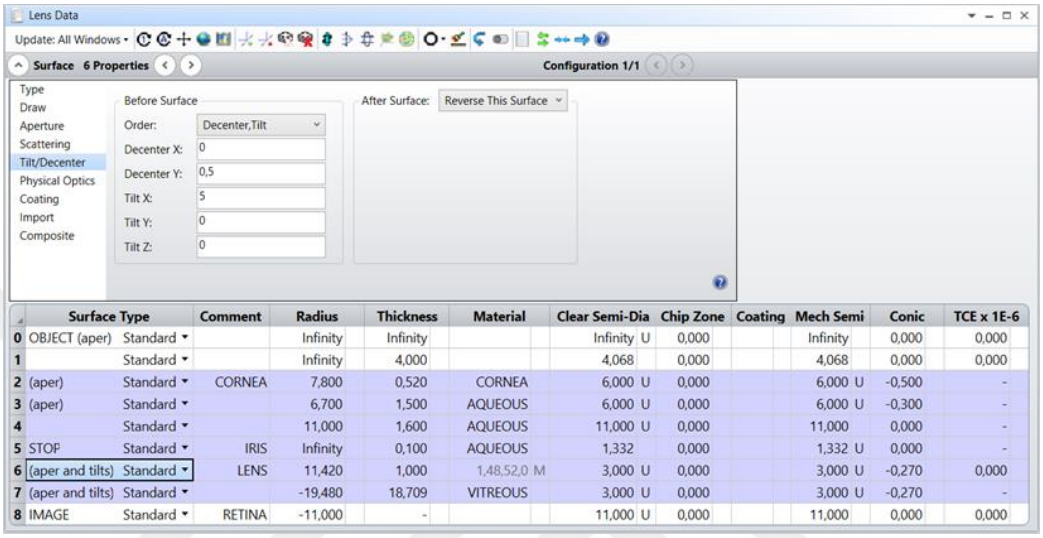

	Surface Type		Comment	Radius	Thickness	Material	Clear Semi-Dia	Chip Zone	Coating	Mech Semi	Conic	TCE x 1E-6
0	OBJECT (aper)	Standard		Infinity	Infinity		Infinity U	0,000		Infinity	0,000	0,000
1		Standard		Infinity	4,000		4,068	0,000		4,068	0,000	0,000
2	(aper)	Standard	CORNEA	7,800	0,520	CORNEA	6,000 U	0,000		6,000 U	-0,500	-
3	(aper)	Standard		6,700	1,500	AQUEOUS	6,000 U	0,000		6,000 U	-0,300	-
4		Standard		11,000	1,600	AQUEOUS	11,000 U	0,000		11,000	0,000	-
5	STOP	Standard	IRIS	Infinity	0,100	AQUEOUS	1,332	0,000		1,332 U	0,000	-
6	(aper and tilts)	Standard	LENS	11,420	1,000	1,48,52,0 M	3,000 U	0,000		3,000 U	-0,270	0,000
7	(aper and tilts)	Standard		-19,480	18,709	VITREOUS	3,000 U	0,000		3,000 U	-0,270	-
8	IMAGE	Standard	RETINA	-11,000	-		11,000 U	0,000		11,000	0,000	0,000

Figure C. 1 Zemax simulation lens data of the aspherical IOL design on the human eye model for 5° tilt and 0.5 decentration.

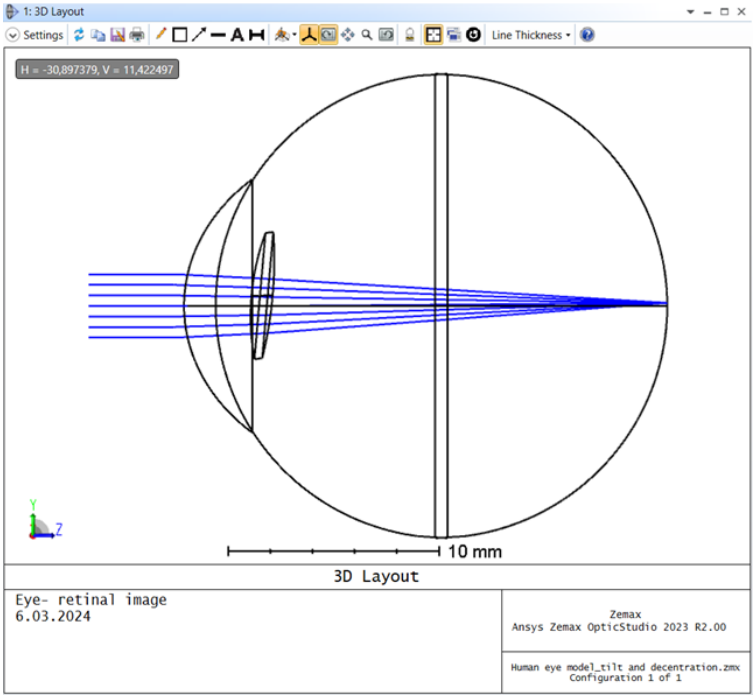

Figure C. 2 Zemax simulation 3D layout of the aspherical IOL design on the human eye model for 5° tilt and 0.5 decentration.

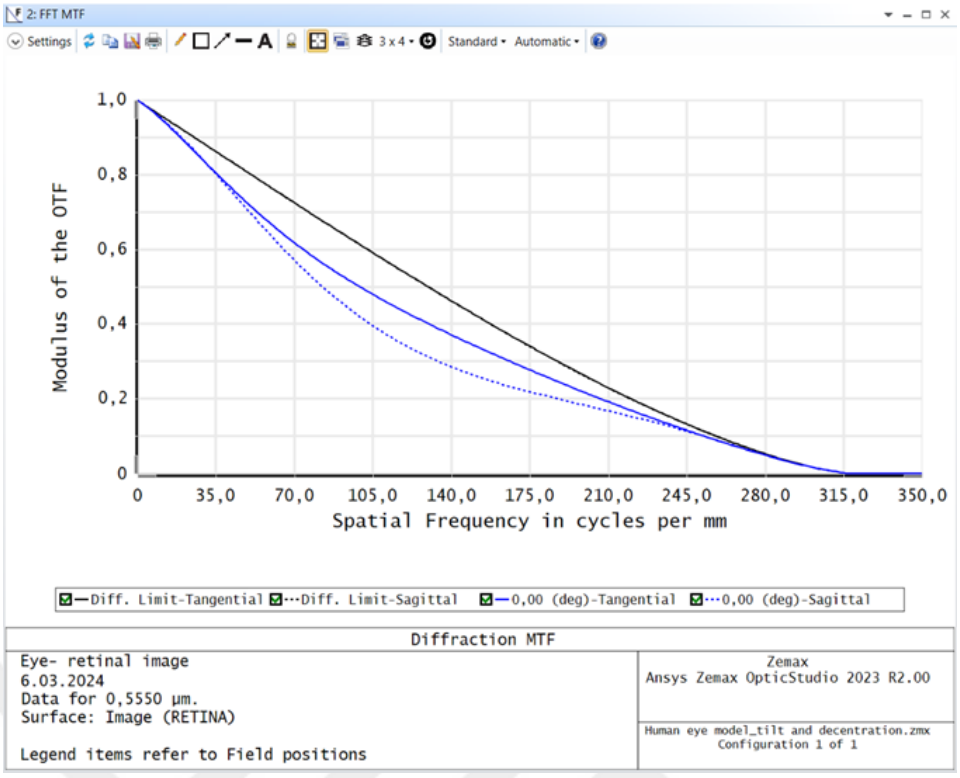

Figure C. 3 Zemax simulation MTF graph of the aspherical IOL design on the human eye model for 5° tilt and 0.5 decentration.

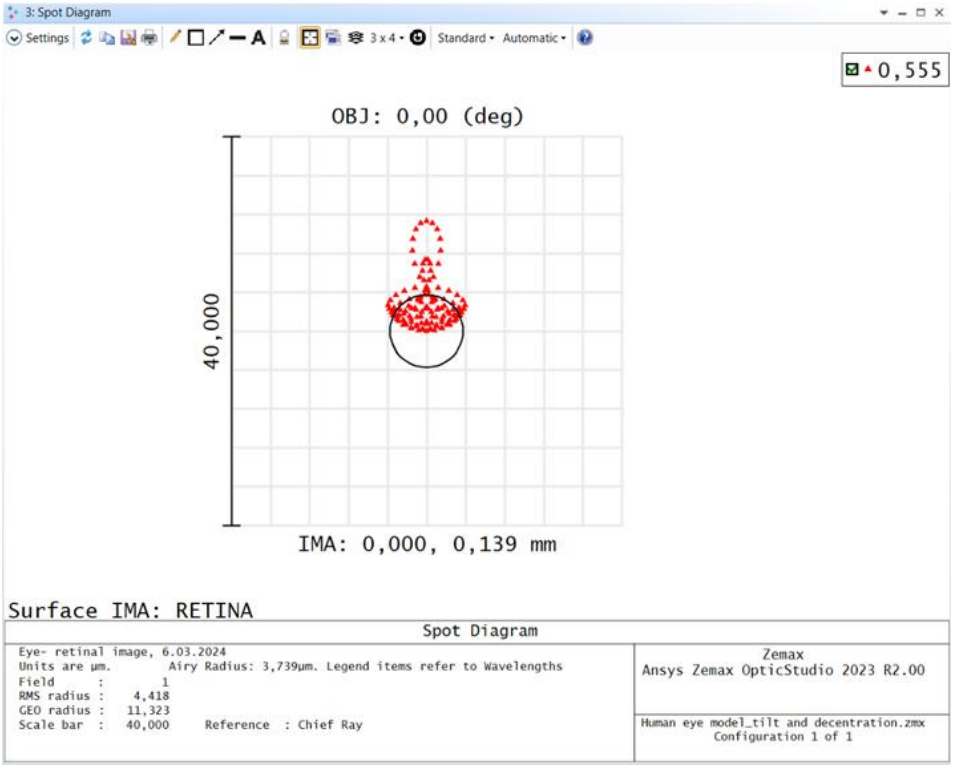

Figure C. 4 Zemax simulation spot diagram of the aspherical IOL design on the human eye model for 5° tilt and 0.5 decentration.

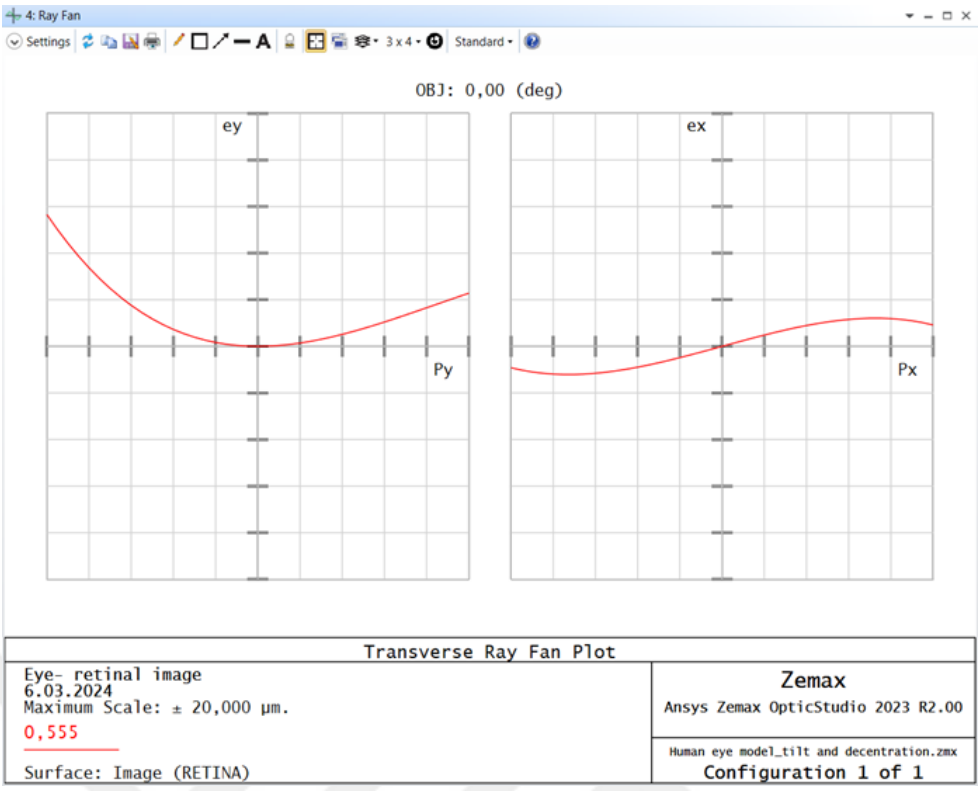

Figure C. 5 Zemax simulation ray fan of the aspherical IOL design on the human eye model for 5° tilt and 0.5 decentration.

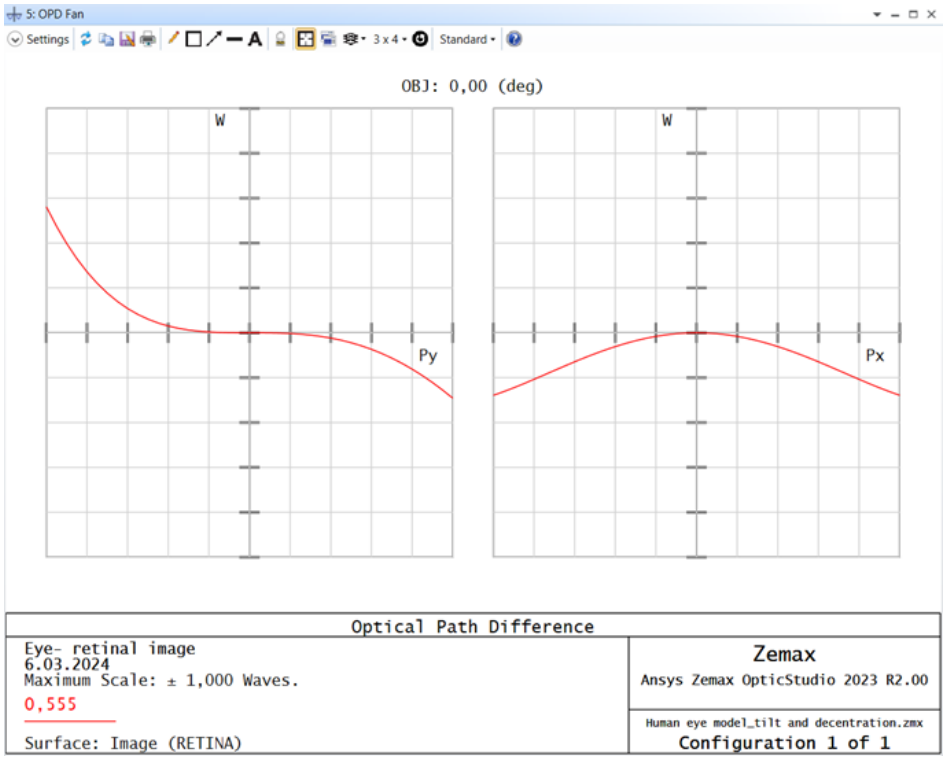

Figure C. 6 Zemax simulation OPD fan of the aspherical IOL design on the human eye model for 5° tilt and 0.5 decentration.

CURRICULUM VITAE

KÜBRA DUMAN

EDUCATION

GAZİANTEP UNIVERSITY

MSc., Optical Engineering (2021-2024)

BSc., Optical and Acoustic Engineering (2014-2019)

ANADOLU UNIVERSITY

BSc., Sociology (2014-2023)

EGE UNIVERSITY

BSc., Mathematics (2011-2014)

EXPERIENCE

- Research & Development Optical Engineer at Biotechnology R&D Center - İstanbul - Turkey (2021-2024)
- Research & Development Engineer at Niki Electronics - İstanbul - Turkey (2020-2021)
- Production and Quality Management Representative at Detay Lighting Company - İstanbul - Turkey (2019-2020)
- Intern Engineer at Arlight Lighting Laboratory – Ankara – Turkey (2018-2019)